MODELING AND CONTROL OF PHOTOVOLTAIC-WIND HYBRID POWER SYSTEM USING A NEURO-FUZZY CONTROLLER

NICHOLAUS JOSEPH MHUSA

MASTERS OF SCIENCE
(Mechatronic Engineering)

JOMO KENYATTA UNIVERSITY OF
AGRICULTURE AND TECHNOLOGY

2016

Modeling and Control of Photovoltaic-Wind Hybrid Power System Using a Neural-Fuzzy Controller

Nicholaus Joseph Mhusa

A thesis submitted in partial fulfillment for the Degree of Master of Science in Mechatronic Engineering in the Jomo Kenyatta University of Agriculture and Technology

2016

DECLARATION

This thesis is my original work and, has not been presented for a degree in any other University.

Signature:..... Date.....

Nicholaus Joseph Mhusa

This thesis has been submitted for examination with our approval as the University Supervisors.

Signature:..... Date.....

Prof George N. Nyakoe

JKUAT, Kenya

Signature:..... Date.....

Dr Erick V. Mgaya

ATC, Tanzania

DEDICATION

This work is dedicated to my wife Mary Kyara and my daughter Michelle Mhusa.

ACKNOWLEDGEMENT

With the will and the help of my Lord, Almighty GOD, I am grateful and thankful from the bottom of my heart for giving me the courage and strength to undertake and complete the goals of this research work. I would like to acknowledge my supervisors, Prof. G. N. Nyakoe and Dr. E.V.Mgaya for their invaluable direction, constructive criticism and advice throughout the research period.

I would like to extend my gratitude to the Arusha Technical College for supporting my studies and providing facilities to conduct my experiments.

I also wish to acknowledge the contributions of my colleagues and fellow post-graduate students in the department of Mechatronic Engineering for their selfless assistance and constructive comments during seminars and conferences.

Thanks to my whole family, especially my lovely wife and parents for their prayers, encouragement, guidance and love which kept me going.

TABLE OF CONTENTS

LIST OF TABLES

LIST OF FIGURES

LIST OF ABBREVIATIONS

AC	Alternating Current
AI	Artificial intelligence
ANFIS	Adaptive Neuro-Fuzzy Inference System
ANN	Artificial Neural Network
Cp	Power Coefficient
DC	Direct Current
FC	Fuel Cell
FL	Fuzzy Logic
FLC	Fuzzy Logic Controller
HS	Hybrid System
HPS	Hybrid Power System
MPP	Maximum Power Point
MPPT	Maximum Power Point Tracking
NFC	Neural Fuzzy Controller
PC	Photovoltaic Cell
PDS	Power Distribution Strategy
PI	Proportional Integral
PID	Proportional Integral Derivatives
PMSM	Permanent Magnet Synchronous Machine
PV	Photovoltaic
RE	Renewable Energy
RES	Renewable Energy Sources
SOC	State Of Charge
SOD	State Of Discharge
SWHPS	Solar Wind Hybrid Power System
TSR	Tip Speed Ratio

NOMENCLATURE

ρ	Air density (kgm^{-}3)
A_m	Area of solar module (m^2)
C_{bat}	Battery bank capacity (Ah)
η_{bat}	Battery efficiency (%)
β	Blade pitch angle
G_t	Global Irradiance (W/m^2)
η_g	Instantaneous PV generator efficiency (%)
η_{inv}	Inverter efficiency (%)
E_L	Load demand (W)
P_m	Mechanical output power of wind turbine (W)
C_p	performance coefficient of wind turbine
E_{PV}	PV Energy (J)
A_s	Swept Area (m^2)
E_{WG}	Wind Generator Energy (J)
V_{wind}	Wind speed (m/s)

ABSTRACT

As energy demands around the world increase, the need for renewable energy sources that will not harm the environment increases. Renewable energy, such as wind and solar energy, is desirable for power generation due to its unlimited existence and environmental friendly nature. However wind and solar sources are not reliable in terms of sustainability and power quality due to their intermittent nature. A management system is thus required for supplying the load power demand. This thesis presents a control strategy for power management in a standalone solar photovoltaic and wind hybrid power system based on artificial intelligence techniques. To ensure efficient optimization of sources, Adaptive Neural Fuzzy Inference System (ANFIS) strategy is employed to achieve the Maximum Power Point (MPP) for photovoltaic (PV) panels and the Fuzzy Logic Control (FLC) strategy is used to achieve the MPP of wind turbine. Moreover, the FLC power management strategy is developed to manage the power flow to the system. The FLC chooses the optimal operating mode of power sources ensuring continuous supply of the load and maintaining the battery state of charge (SOC) at acceptable levels. The proposed system and its control strategy was assessed using a hybrid system comprising of PV panels, wind turbine and battery storage. Perturb and observe (P&O) MPP algorithm is used for a comparison with the proposed ANFIS MPPT system. From the simulation results based on the mathematical model of the system, the comparison of proposed MPPT with the classical P&O reveals the robustness of the proposed PV control system for solar irradiance and temperature changes. Moreover results also show that the proposed FLC Power management strategy for the hybrid system gives a greater reliability in terms of power generation and distribution compared to a stand alone system with single source. It provides effective utilization of power sources and minimizes usage of the battery, hence improving its life. The whole system is analyzed through simulation in MATLAB / Simulink environment.

CHAPTER ONE

INTRODUCTION

1.1 Background

Social, economic and industrial growth of any country requires energy. Fossil fuels are the major energy sources, which have been over- utilized leading to disastrous effects such as air pollution and destruction of the environment. Burning of fossil fuels releases harmful gases, that have severe consequences on the habitats and also affect human health [1]. They are non-renewable sources of energy as they are derived from pre-historic fossils and are no longer available once used. Their source is limited and they are being depleted at a faster rate. Renewable energy generation is a good option for protecting the environment as well as a solution towards the limited availability of fossil fuel.

The increasing energy demand, high energy prices, as well as concerns over environmental effect, health and climate change, have attracted many researchers and communities to move into alternative energy studies. Many studies have been done to make use of renewable energy sources (e.g. solar,biogas and wind) that are stand alone [2], [3]. Among these, solar and wind energy are two of the most promising renewable power generation technologies. Solar power or wind power is normally used by remote off-grid areas where mains electricity supply is unavailable. The disadvantage of standalone power systems using renewable energy sources is that their availability is affected by daily and seasonal patterns which results in difficulties in regulating the output power to the load [4]. For example, fluctuating daily wind speeds and solar irradiation cut-off at night and cloudy days, leads to solar and wind systems with low reliability in supplying the load throughout a day. Since neither solar power nor wind power is available

constantly throughout the day, month or year, exclusive solar or wind power systems cannot be used on standalone basis for electrical installations which require constant guaranteed power. A good alternative to this is the use of hybrid energy systems [1].

A major limitation for these hybrid systems is the control requirement for optimal efficiency [5]. Conventional control algorithms require a mathematical model for the dynamic system to be controlled. The mathematical model is then used to construct a controller. In many practical situations, however, it is not always feasible to obtain an accurate mathematical model of the controlled system. Artificial intelligence (AI) control offers a way of dealing with problems that are difficult to model by implementing linguistic, non-formal control laws derived from expert knowledge [6]. Fuzzy logic control systems have benefits of replicating all desired features of human input, while maintaining all the advantages of closed-loop automatic control. One of the major problems in the use of the fuzzy logic control is the difficulty of choice and design of membership functions to suit a given problem [6]. A systematic procedure for choosing the type of membership function and the ranges of variables in the universe of discourse is still not available. Tuning of the fuzzy controller by trial and error is often necessary to get a satisfactory performance. However, neural networks have the capability of identifying the characteristic features of a system that can be extracted from the input-output data. This learning capability of the neural network can be combined with the control capabilities of a fuzzy logic system resulting in a neuro-fuzzy inference system [6].

Control of hybrid power systems tends to be a complex task, given that such systems cannot be accurately modeled as they are composed of a large number of variables. Various methods for power optimization and management have been reported in literature. The existing methods have drawbacks in terms of

efficiency, accuracy and flexibility. Thus there is a need for developing a controller which will overcome these drawbacks. This research explored ways of improving efficiency and proper management of power flow in a PV-Wind hybrid system using artificial intelligence techniques.

1.2 Problem statement

The integration of different types of energy sources (e.g. PV, wind, biogas and diesel) and storage media in a hybrid system has resulted in complex supply structures. One of the challenges facing such complex systems is the control requirement for optimal efficiency. The batteries in these stand-alone systems are the most sensitive equipment and often operate under severe conditions (such as excessive charge/discharge and long periods under deep and partial discharge conditions). Therefore, the battery life in PV stand-alone systems is within 2-4 years, which is very short compared to the manufacturer's defined life-time of the PV generator which has a life-time of approximately 20 years [7]. Therefore there is a need to develop a controller which should be able to take decision intelligently on different parameters like availability of power, variation in load and different battery condition

1.3 Objectives

The main objective of this research is to design,simulate and evaluate an intelligent controller for optimizing the power generated by sources, with capability to properly manage power flow between photovoltaic-wind hybrid power system and energy storage element(s).

To achieve the above objective, the following were the specific objectives.

1. To develop a neural-fuzzy model for PV-Wind hybrid power system based on manufacturer's specifications and validate it experimentally.

2. To develop a control algorithm for optimal power flow management of the PV-Wind hybrid power system.

3. To carry out simulation and evaluate the performance of the PV-Wind hybrid power system.

1.4 Justification of the study

It has been demonstrated that PV-Wind hybrid energy systems can significantly reduce the total life cycle cost of stand-alone power supply, while at the same time providing a more reliable supply of electricity [8]. However, due to the high nonlinearities characterizing the PV-Wind hybrid system, it would be impractical to develop a rigorous mathematical model and, at the same time, obtain a simple and effective controller for the system. Nowadays, considerable attention has been focused on use of artificial neural networks (ANN) and fuzzy logic control (FLC) on system modeling and control applications. Neural networks, with their remarkable ability to derive meaning from complicated or imprecise data, can be used to extract patterns and detect trends which are too complex to be noticed by either humans or other computer techniques. This research applies neural-fuzzy control techniques for solving the PV-Wind hybrid power system efficiency optimization problem. The controller will protect the battery against overcharge and over discharge hence prolonging the battery life. Moreover, the controller will achieve the coordination between the components of a PV-Wind hybrid system as well as control the energy flows.

1.5 Scope

The thesis focuses on power optimization strategy for PV system used as the main energy generator in the hybrid system. It also deals with power optimization strategy used in wind turbine power system. Last but not least focus on power management for the hybrid system comprising of PV system, Wind system and Energy Storage which used to store energy and to reduce the output power fluctuation.

1.6 Outline of the Thesis

This thesis contains six chapters. The first chapter provides an introduction to the research by highlighting the existing problems, the objective and the scope of the research work. Chapter 2 is a review of literature on elements of the hybrid PV-Wind system. It provides useful information about photovoltaic (PV) power system, wind turbine power system and hybrid photovoltaic/wind power system relevant to this study. Chapter three gives the methodology for modeling PV-Wind power system. The chapter discusses the MATLAB/Simulink block modeling for the photovoltaic, wind and hybrid power systems. The Simulink block for the entire system was developed and simulated separately before obtaining the combined system. Chapter 4 gives the methodology showing the process used to design the controller for energy optimization and distribution. Chapter 5 presents the results and their discussion. The conclusion and recommendations for further work are made in Chapter 6.

CHAPTER TWO

LITERATURE REVIEW

2.1 Overview

Energy plays an important role in our daily life activities as there is a large increase in population, urbanization and industrialization. The major fossil fuels like coal, petroleum and natural gas are getting depleted and it is expected that they will be exhausted in a few hundred years. To meet future energy requirements, alternative or renewable sources of energy, e.g solar and wind, are needed. Solar and wind energy systems are taking the biggest share to mitigate this situation [5] . To increase power supply reliability, solar and wind energy are used as dual energy sources. However, a drawback common to solar and wind options, is their unpredictable nature and dependence on weather and climatic changes, and the variations of solar and wind energy may not match with the time distribution of load demand [7]. This shortcoming not only affects the system's energy performance, but also results in batteries being discarded too early. Therefore there is a need to improve the energy supply reliability by optimizing the energy produced by solar and wind hybrid systems. Moreover, managing flow of energy throughout the hybrid system is essential to enable continuous energy flow.

This chapter presents information about the background studies on PV power system, wind power system and hybrid power system. It gives an overall idea on developing, modeling, optimization and control technologies for hybrid PV-Wind system. Moreover, challenges that have been faced in wind/solar energy conversion and some of the solutions that have been proposed are also presented. A summary of the research gaps identified is given at the end of the chapter with a proposed approach to fill the gap.

2.2 Photovoltaic Energy Conversion

A photovoltaic system converts sunlight into electricity. The basic element of a photovoltaic system is the photovoltaic cell [9]. Cells may be grouped to form panels or modules. Panels can be grouped to form large photovoltaic arrays. The term array is usually employed to describe a photovoltaic panel (with several cells connected in series and/or parallel) or a group of panels as shown in Figure 2.1. Panels connected in parallel increase the current and connected in series provide a greater output voltage [9].

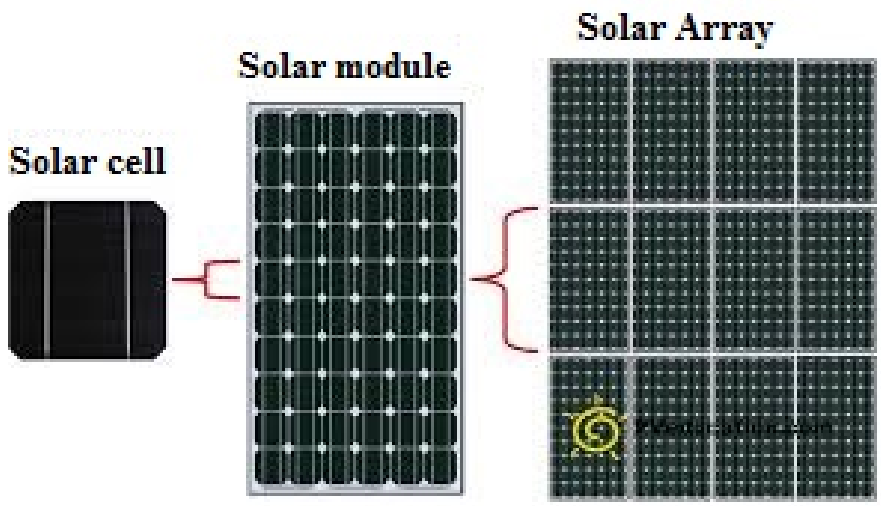

Figure 2.1: Photovoltaic cell, module and array

Solar cells are made from semiconductor materials that are able to generate electric current when being exposed to sunlight radiation. When a photon (particle of light) strikes a photovoltaic cell, some of the energy it brings is captured by the semiconductor material. That energy knocks electrons, allowing them to flow freely. Electric fields created between the positive layer (P-type) and the negative layer (N-type) of the cells then force the loose electrons to go in a certain direction through a connecting wire as direct current (DC) electricity. The entire conversion process is illustrated in Figure 2.2 [10].

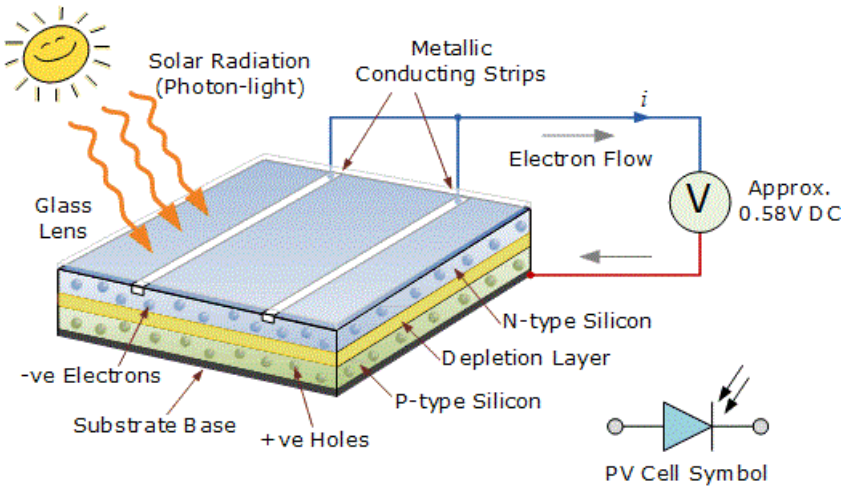

Figure 2.2: Schematic Block Diagram of PV Cell

The performance of a PV array system depends on the operating conditions as well as the solar cell and array design quality. The output voltage, current and power of a PV array vary as functions of solar irradiation level, temperature and load current [11]. Therefore the effects of these three quantities must be considered in the design of PV arrays so that any change in temperature and solar irradiation levels should not adversely affect the PV array output to the load/utility, which is either a power company utility, grid or any stand alone electrical type load.

Modeling of Photovoltaic Module

Reliable knowledge and understanding of the PV module performance under different operating conditions is of great importance for correct product selection and accurate prediction of its energy performance. The performance of a crystalline silicon PV module is a function of the physical variables of the PV module material, temperature of PV module and the solar radiance on the PV module surface [11].

For engineering application, many researchers have investigated the simplified

simulation models, such as the power efficiency models [12], which can predict the time series or average performance of a PV array under variable climatic conditions.

Kerr and Cuevas [12] presented a new technique, which can determine the current–voltage (I–V) characteristics of PV modules based on simultaneously measuring the open-circuit voltage as a function of a slowly varying light intensity. They have also given a detailed theoretical analysis and interpretation of such quasi-steady-state open circuit voltage (Voc) measurements. Borowy and Salameh [13] gave a simplified model with which the maximum power output could be calculated for a PV module once solar radiation on the PV module and ambient temperature were found.

Zhou et al. [14] presented a novel simulation model for PV array performance predictions for engineering applications based on the I-V curves of a PV module. Five parameters are introduced to account for the complex dependence of PV module performance upon solar radiation intensities and PV module temperatures. The authors concluded that this simulation model is simple and especially useful for engineers to calculate the actual performance of the PV modules under operating conditions, with limited data provided by the PV module manufacturers. Yang et al. [23] developed one model for calculating the maximum power output of PV modules according to the theory of equivalent circuit of solar cells by using eight parameters which can be identified by regression with the Amoeba Subroutine or Downhill Simplex Method from experimental data. Accuracy of this model was validated by experimental data with good fitness.

The mathematical model for estimating the power output of PV module based on the equivalent circuit of solar cells is described next.The equivalent circuit of a PV cell is shown in Figure 2.3. It includes a current source, a diode, a series resistance and a shunt resistance [2], [9].

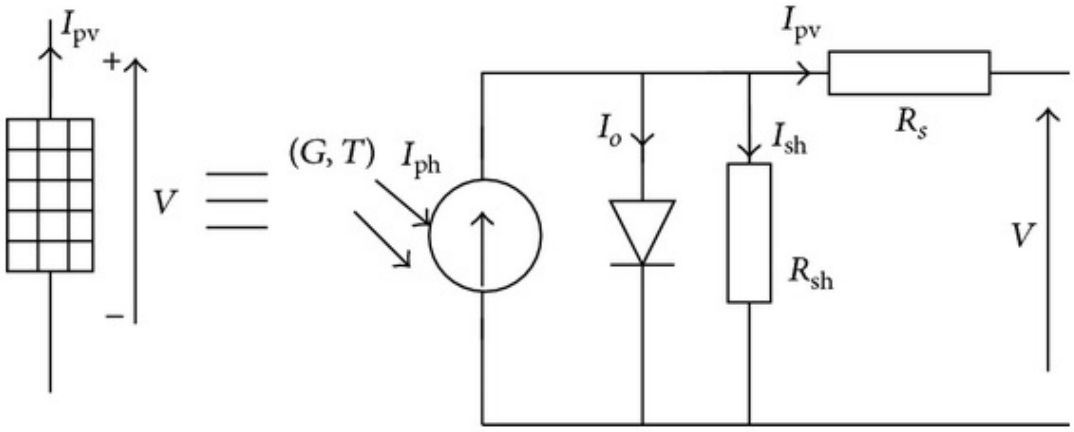

Figure 2.3: Equivalent circuit of a PV cell

The current source I_{ph} represents the cell photocurrent. R_{sh} and R_s are the intrinsic shunt and series resistances of the cell, respectively. Usually the value of R_{sh} is very large and that of R_s is very small, hence they may be neglected to simplify the analysis. PV cells are grouped in larger units called PV modules which are further interconnected in a parallel-series configuration to form PV arrays. The photovoltaic module can be modeled mathematically as given in the following equations:

Module photo-current is given by:

$$I_{ph} = [I_{SCr} + K_i(T - 298)].G/1000 \tag{2.1}$$

where I_{ph} is the light generated current in a PV module (A), I_{SCr} is the PV module short-circuit current at 25^oC and 1000W/m^2, K_i is the short-circuit current temperature co-efficient at $I_{SCr} = 0.0017A/^oC$, T is the module operating temperature in Kelvin, G is the PV module illumination $(W/m2)$ = 1000W/m^2.

Module reverse saturation current, I_{rs}, is given by:

$$I_{rs} = \frac{I_{SCr}}{[exp^{(qVoc/NskAT)} - 1]} \tag{2.2}$$

where q is electron charge $= 1.6\times10^{-19}C$, Voc is the open circuit voltage, Ns is the number of cells connected in series, k is Boltzman constant $= 1.3805 \times 10^{-23}J/K$,

$A = B$ is an ideality factor = 1.6,

The module saturation current I_0 varies with the cell temperature, which is given by:

$$I_o = I_{rs}[\frac{T}{T_r}]^3 exp\left[\frac{q.E_{go}}{B_k}\left[\frac{1}{T_r} - \frac{1}{T}\right]\right] \tag{2.3}$$

where T_r is the reference temperature = 298 K, I_o is the PV module saturation current (A), E_{go} is the band gap for silicon = 1.1 eV.

The current output of PV module is

$$I_{pv} = N_p.I_{ph} - N_p.I_o[exp\left[\frac{q.(V_{pv} + I_{pv}Rs)}{N_s A_k T}\right] - 1] \tag{2.4}$$

Where N_p is the number of cells connected in parallel, V_{pv} is output voltage of a PV module (V), I_{pv} is output current of a PV module (A), Rs is the series resistance of a PV module. Equations (2.1) - (2.4) are used to develop the PV model.

Maximum Power Point Tracking of Photovoltaic Module

A typical solar panel can convert only 30 to 40 percent of the incident solar irradiation into electrical energy. Maximum power point tracking technique is used to improve the efficiency of the solar panel. Therefore, the MPP of a photovoltaic array is an essential part of a PV system. As such, many maximum power point tracking (MPPT) techniques have been developed and implemented [15]. Among these techniques, hill-climbing MPPT such as perturb and observe (P&O) [15] was used by many researchers. (P&O) is a simple algorithm that does not require previous knowledge of the PV generator characteristics and is easy to implement with analogue and digital circuits. In this technique, first the PV voltage and current are measured and then the corresponding power $P1$ is calculated. Considering a small perturbation of voltage (ΔV) or perturbation of duty cycle (ΔP) of the dc-dc converter in one direction, the corresponding power $P2$ is calculated.

$P2$ is then compared with $P1$. If $P2$ is more than $P1$, then the perturbation is in the correct direction; otherwise it should be reversed. In this way, the peak power point is tracked and hence the corresponding voltage can be calculated [16] [17]. The major drawbacks of P&O/ (hill-climbing) are occasional deviation from the maximum operating point in case of rapidly changing atmospheric conditions, such as broken clouds. Also, correct perturbation size is important in providing good performance in both dynamic and steady-state response [18]. In addition, P&O technique may cause many oscillations around the MPP, and this slows down the response of the system.

Introduction of intelligent MPPTs in PV systems has been very promising. These algorithm achieve very good performances, fast responses with no overshoot, and less fluctuations in the steady state for rapid temperature and irradiance variations [15]. FL-based MPPTs do not require the knowledge of the exact PV model [19], [20]. Artificial Neural Network (ANN)-based MPPT technique operates like a black box model, requiring no detailed information about the PV system [20]. For Maximum Power Point Tracking, ANN input can be PV array parameters like PV voltages and currents, environmental data like irradiance and temperature, or any combination of these, whereas the output signal is the identified maximum power or the duty cycle signal used to drive the electronic converter to operate at the MPP. The ANN input and output data are obtained from experimental measurement or model-based simulation results. After learning the relation between temperature and irradiance,an ANN can track the MPP online [20].

In this research, an intelligent control technique based on ANN is used together with an MPPT controller in order to increase the tracking response and consequently increase the tracking efficiency of the solar panel. The neural network control (NNC) has two inputs; the solar irradiance and temperature. NNC is

used to estimate the PV panel operating voltage (Vref) which corresponds to the maximum power (Pmax) at any given solar irradiation and cell temperature.

2.3 Wind Energy Conversion

Wind turbine is an important element in a wind power system to generate electricity. It consists of a rotor mounted to a nacelle and a tower with two or more blades mechanically connected to an electric generator. The gearbox in the mechanical assembly transforms slower rotational speeds of the wind turbine to higher rotational speeds on the electric generator. The rotation of the electric generator's shaft generates electricity whose output is maintained by a control system. Currently, two types of configurations for wind turbine exist, which are the vertical-axis wind turbine (VAWT) configuration and the widely used horizontal-axis wind turbine (HAWT) configuration. HAWT has the ability to collect maximum amount of wind energy for a given time of day and season and their blades can be adjusted to avoid high wind storm [21]. Wind turbines operate in two modes namely constant or variable speed. For a constant speed turbine, the rotor turns at constant angular speed regardless of wind variations. One advantage of this mode of operation is that it eliminates the use of expensive power electronic converters, [3]. Its disadvantage however, is that it constrains rotor speed so that the turbine cannot operate at its peak efficiency in all wind speeds. For this reason, a constant wind speed turbine produces less energy at low wind speeds than does a variable wind speed turbine which is designed to operate at a rotor speed proportional to the wind speed below its rated wind speed [21]. The output power or torque of a wind turbine is determined by several factors. These include turbine speed, rotor blade tilt,rotor blade pitch angle size and shape of turbine, area of turbine, rotor geometry whether it is a HAWT or a VAWT, and wind speed [22]. A relationship between the output power and the various variables constitute the mathematical model of the wind turbine. In

this research a model describing Horizontal Axis Wind Turbine (HAWT) was used to develop a controller that optimize power generated by wind turbine.

Modeling of Wind Turbine

Different wind generators have different power output performance curves. Therefore, the model used to describe the performance of wind generators is expected to be different. Choosing a suitable model is very important for wind turbine power simulations, it is a pre-requisite for the successful planning and implementation of wind power generation projects. The hour-by-hour simulation programs have been the main tools to determine the long-term performance of wind energy systems. Based on the hourly wind speed data, the long-term performance of the wind system can be obtained. The power output characteristic of the wind turbine is shown in Figure 2.4.

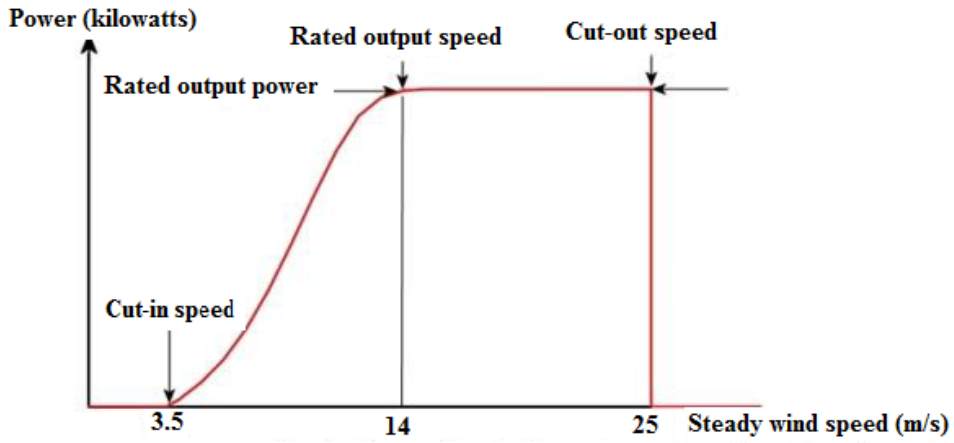

Figure 2.4: Wind turbine power output with steady wind speed

At very low wind speeds, there is insufficient torque exerted by the wind on the turbine blades to make them rotate. However, as the speed increases, the wind turbine will begin to rotate and generate electrical power. The speed at which the turbine first starts to rotate and generate power is called the Cut-in

speed and is typically between 3 and 4 metres per second. As the wind speed rises above the cut-in speed, the level of electrical output power rises rapidly as shown. However, typically somewhere between 12 and 17 metres per second, the power output reaches the limit that the electrical generator is capable of. This limit to the generator output is called the Rated output power and the wind speed at which it is reached is called the rated output wind speed. At higher wind speeds, the design of the turbine is arranged to limit the power to this maximum level and there is no further rise in the output power. How this is done varies from design to design but typically with large turbines, it is done by adjusting the blade angles so as to to keep the power at the constant level. As the speed increases above the rated output wind speed, the forces on the turbine structure continue to rise and, at some point, there is a risk of damage to the rotor. As a result, a braking system is employed to bring the rotor to a standstill. This is called the Cut-out speed and is usually around 25 meters per second [21].

Based on the above assumptions, the most simplified model to simulate the power output of a wind turbine is described by [23]. In other case studies [24] [25], a similar model is applied regarding the Weibull shape parameter. Additionally, there are other types of models to describe the power output of wind turbines, where the quadratic expressions are applied for the simulation [26]. However, it is generally acknowledged that the hour-by-hour simulation programs require hour-by-hour wind speed data, which may not be available for many locations. Therefore, some simplified design algorithms [27] have been developed as alternatives to simulation programs to determine the long-term performance of renewable energy systems. However, it is generally acknowledged that if the simulation model is more general, it is usually less accurate.

In some other researches, calculation of wind turbine power is based on electrical load, average wind speed and power curve of the wind turbine [28]. Since

the calculation based on actual wind speed and direction is time-consuming and sometimes impossible, average wind speed can be used. Sometimes, the wind turbine power curves cannot exactly represent wind turbine power output because the curves can only give the power output of the wind turbine as a function of the average wind speed, ignoring instantaneous wind speed variations, and thereby will, to some extent, undermine the performance of the wind turbine [29]. Therefore, considering the effect of instantaneous variations of wind speed for a hybrid system can improve the accuracy whereas considering actual wind speed for a hybrid system is almost impossible. Zamani and Riahy [30] presented a new method for calculating the power of a wind turbine by considering wind speed variations. The rate of wind speed variations is assessed by the energy pattern factor (EPF) of actual wind, and the performance of rotor speed and pitch angle controllers is evaluated by a new factor, named wind turbine controllability (Ca). By using the EPF and Ca, the power curve is modified by considering the extra power that is captured by the controllers. The mathematical formulation of turbine model considering the variation of wind speed is described next.

For an object having mass m and velocity v_w under a constant acceleration, the kinetic energy W_w is given by

$$W_w = \frac{1}{2} m v_w^2 \tag{2.5}$$

The mechanical power P_m in the wind is given by the rate of change of kinetic energy, i.e

$$P_w = \frac{dW_w}{dt} = \frac{1}{2} \frac{dm}{dt} v_w^2 \tag{2.6}$$

But mass flow rate $\frac{dm}{dt}$ is given by

$$\frac{dm}{dt} = \rho A v_w \tag{2.7}$$

where A is the swept area of the turbine and ρ is the density of air. With this expression, Equation 2.7 becomes

$$P_m = \frac{1}{2} \rho A v_w^3 \tag{2.8}$$

The actual mechanical power P_m extracted by the rotor blades, in watts, is the difference between the upstream and the downstream wind powers [3], i.e.

$$P_m = \frac{1}{2}\rho A v_w (v_u^2 - v_d^2) \tag{2.9}$$

where v_u is the upstream wind velocity at the entrance of the rotor blades in m/s and v_d is the downstream wind velocity at the exit of the rotor blades in m/s. From the mass flow rate, Equation 2.7 can be written as

$$\rho A v_w = \frac{\rho A (v_u + v_d)}{2} \tag{2.10}$$

v_w being the average of the velocities at the entry and exit of rotor blades of turbine. With this expression, Equation 2.10 can be simplified and becomes

$$P_m = \frac{1}{2} C_p(\lambda, \beta) \rho A v_w^3 \tag{2.11}$$

C_p is performance coefficient of the turbine (also known as power coefficient). The power coefficient represents a fraction of the power in the wind captured by the turbine and has a theoretical maximum of 0.593. c_p is often called the Betz limit after the Germany physicist Albert Betz who worked it out in 1919 [22]. The power coefficient can be expressed by a typical empirical formula as

$$C_p = \frac{1}{2}(\lambda - 0.022\beta^2 - 5.6)e^{-0.17\lambda} \tag{2.12}$$

where β is blade pitch angle (deg) and λ is the tip speed ratio of the turbine, defined as

$$\lambda = \frac{r_m \omega_b}{v_w} \tag{2.13}$$

where w_b is the turbine angular speed (rad s^{-1}) and r_m is turbine radii(m). The mechanical power generated by the turbine rotor to the initial power of the wind turbine power coefficient Cp say that a non-linear relationship between the tip speed and blade pitch angle. Figure 2.5. shows that at different blade angle, the power coefficients vary with tip speed ratio. From Figure 2.5, it can be seen that the variation of power coefficient versus the blade pitch angle β. Where the

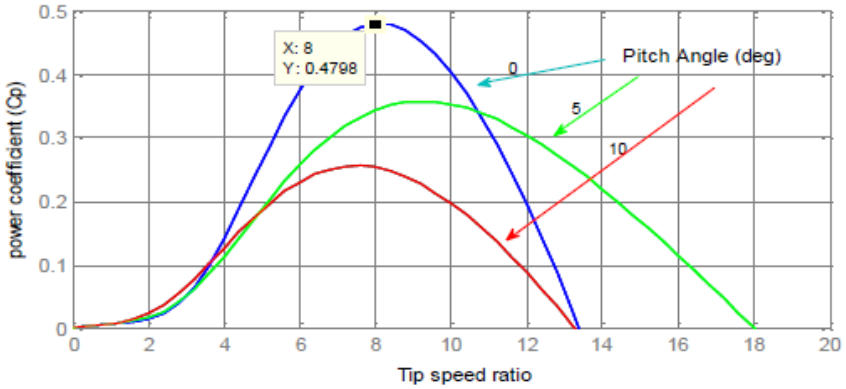

Figure 2.5: Power coefficient characteristics of a wind turbine.

β gradually increases, the curve of Cp will decrease significantly. Generally, to achieve the maximum wind power, β value should be very small. If β is at a given value, then Cp has a maximum value $Cpmax$.

Maximum Power Point Tracking of Wind Turbine

According to Equation 2.11, the most important parameters to achieve the maximum power point of wind turbine is Cp curve, so that maximum power output of wind turbines occurs when Cp is maximum. From the graph, at a constant β, the optimum Cp occurs at different values of λ. So if the wind speed is considered constant, Cp value will depend on the wind turbine rotor speed. Thus, by controlling the rotor speed, turbine power output is controlled. In addition, for each specific wind speed, there is only one rotor speed which leads to maximum power. Figures 2.6 and 2.7 show the curves of the wind turbine power- rotor speed and turbine torque – rotor speed for the different wind speeds. From the figures, it is clear that for the different power curves, the maximum powers are achieved at the different rotor speeds. Therefore, the rotor speed should be operated at the optimum speed. This technique is called as MPPT (Maximum Power Point Tracking).

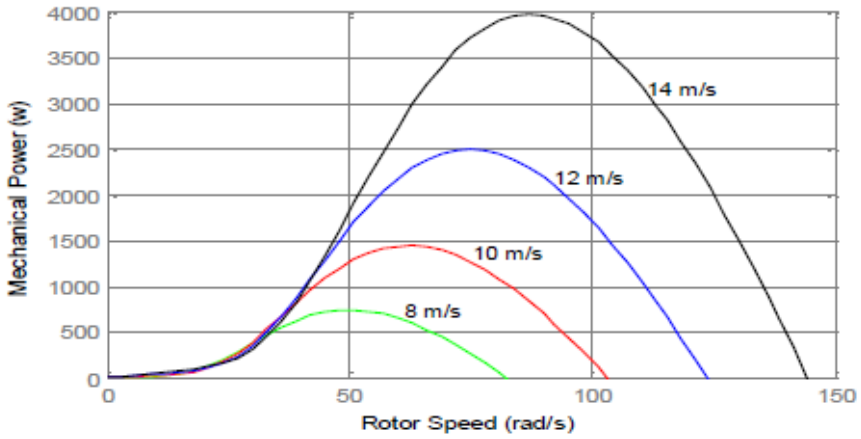

Figure 2.6: The power curves for different wind speeds and zero pitch angle

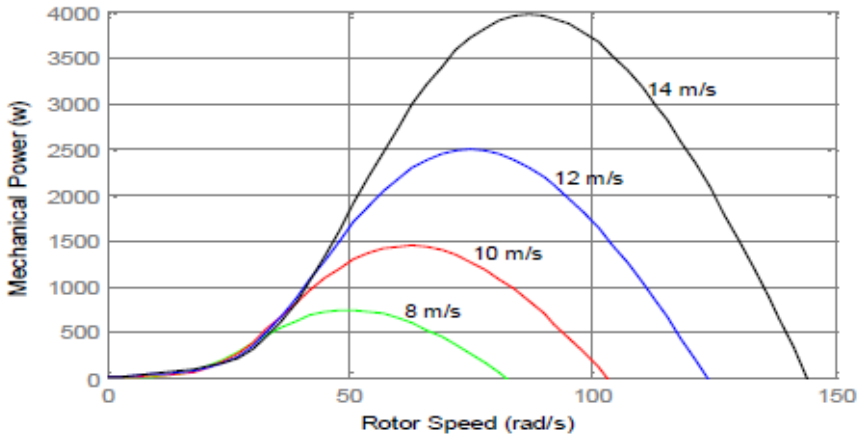

Figure 2.7: The Torque curves for different wind speeds and zero pitch angle

2.4 Energy Storage System

The harnessing of renewable energies presents, however, a further set of technical and economic problems. Unlike fossil and nuclear fuels, which are concentrated sources of energy that can be easily stored and transported, renewable forms of energy are highly dilute and diffuse [31]. Moreover, their supply can be extremely intermittent and unreliable. So, batteries are required to even out irregularities in the solar and wind power distributions. The development of battery behavior

models has been the focus of researchers for many years [31]. Based on the model given by Cugnet and Liaw [32] and incorporation of the diffusion precipitation mechanism studied by Oliveira and Lopes [33] in the reaction kinetics of the negative electrode, Kim and Hong [34] analyzed the discharge performance of a flooded lead acid battery cell using mathematical modeling. Bernardi and Carpenter [35] developed a mathematical model of lead acid batteries by adding the oxygen recombination reaction. Nguyen et al. [36] presented a model analogous to the flooded type and examined the dynamic behavior of the cell during discharge with respect to cold cranking amperage and reserve capacity. In general, these models are complex in terms of the expressions and number of parameters employed. Yang et al. [8] states that a lead acid battery is characterized by two indexes, i.e. the state of charge (SOC) and the floating charge voltage (or the terminal voltage). Extensive SOC determination methods have been introduced by Sabine Piller et al. [37]. It concluded that the most used modeling technique at this time for all systems is ampere-hour counting method because it is the most direct and transparent method and quite easily implemented with satisfyingly accurate results for short- time applications, especially if used in the range of low to medium SOC. The lead-acid battery is used in this thesis for energy storage. The section below describes the mathematical formulation of lead acid battery model based on its state of charge.

Modeling of Battery Storage

At any hour, the state of battery is related to the previous state of charge and to the energy production and consumption situation of the system during the time from $t-1$ to t. During the charging process, when the total output of PV and wind generators is greater than the load demand, the available battery bank

capacity at hour t can be described by [38];

$$C_{bat}(t) = C_{bat}(t-1) * (1-\sigma) + \Big(E_{pv}(t) + E_{WG}(t) - \frac{E_L(t)}{\eta_{inv}}\Big)\eta_{bat} \tag{2.14}$$

where $C_{bat}(t)$ and $C_{bat}(t-1)$ are the available battery bank capacity (Wh) at hour t and $t-1$, respectively, η_{bat} is the battery efficiency (during discharging process, the battery efficiency = 1), σ is self-discharge rate of the battery bank; $E_{pv}(t)$ and $E_{WG}(t)$ are the energy generated by PV and wind generators, respectively; $E_L(t)$ is the load demand at hour t and η_{inv} is the inverter efficiency (%).

On the other hand, when the load demand is greater than the available energy generated, the battery bank is in discharging state. Therefore, the available battery bank capacity at hour t can be expressed as:

$$C_{bat}(t) = C_{bat}(t-1) * (1-\sigma) - \Big(\frac{E_L(t)}{\eta_{inv}} - (E_{pv}(t) + E_{WG}(t))\Big) \tag{2.15}$$

At any hour, the storage capacity is subject to the following constraints:

$$C_{batmin} \leq C_{bat}(t) \leq C_{batmax} \tag{2.16}$$

2.5 The Power Conditioning Unit

To connect a photovoltaic or wind turbine to an external system, it is necessary to boost its voltage or to increase its number [8]. Therefore, a boost converter is used. A boost converter is a class of switching-mode power supply containing at least two semiconductor switches and at least one energy storage element. In addition, a capacitor is often added to the converter output to reduce the ripple of its output voltage as shown in Figure 2.8

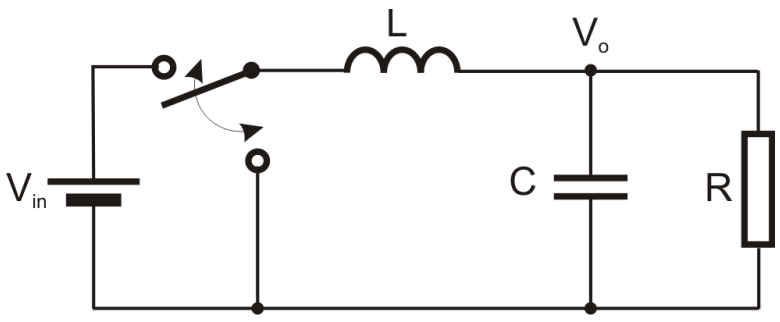

Figure 2.8: Schematic of DC-DC Boost converter

Equation 2.17 describes the relation between the input and the output voltage of a boost converter as a function of the duty cycle D.

$$\frac{Vout}{Vin} = \frac{1}{1-D} \tag{2.17}$$

2.6 Hybrid Systems

One of the main problems with solar and wind energy is their intermittent nature and the resulting discontinuity in delivery of power. Such problems can be mitigated by the use of hybrid technologies that involve utilization of more than one energy resource and converting all of them into a single energy form [39]. A few examples would be wind/PV electric systems, wind/diesel generator system, Wind/PV/Hydro system and PV/Wind/Biogas system [39]. Figure 2.9 shows a typical hybrid system consisting of PV and Wind. A typical hybrid energy system would consist of:

1. A primary source of energy, typically a renewable energy resource.
2. A secondary source of energy for supplying power in case of shortages, i.e. a diesel generator, Fuel cell or battery.
3. A storage system for a stable power output, i.e. battery system.
4. A charge controller to regulate the current through the battery.

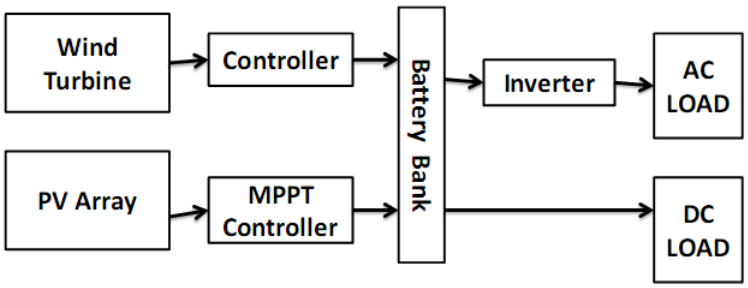

Figure 2.9: Hybrid system consisting of PV and Wind sources

2.7 Modeling of hybrid solar-wind system components

A hybrid solar–wind system consists of PV array, wind turbine, battery bank, inverter, controller, and cables. The PV array and wind turbine work together to satisfy the load demand. When the energy sources (solar and wind energy) are abundant, the generated power, after satisfying the load demand, will be supplied to feed the battery until it is fully charged. On the other hand, when energy sources are low, the battery will release energy to assist the PV array and wind turbine to cover the load requirements until the storage is depleted.

The hybrid solar–wind system design is mainly dependent on the performance of individual components. In order to predict the system's performance, individual components should be modeled first and then their combination can be evaluated to meet the demand reliability. If the power output prediction from these individual components is accurate enough, the resultant combination will deliver power at the least cost [42].

2.8 System Control for Energy Flow in PV-Wind Hybrid System

One main problem for the hybrid solar–wind system is related to the control of the energy distribution. The dynamic interaction between the renewable energy sources and the load demand can lead to critical problems of stability and power quality that are not very common in conventional power systems. Managing flow of energy throughout the proposed hybrid system to assure continuous power supply for the load demand is essential. Conventional approaches for controlling power supply to the load requirement according to the demand was used in var-

ious hybrid systems [42]. In the conventional approach, power electronics based DC–DC converters are used for maximum energy extraction from solar and wind energy resources, and to control the complete hybrid system.

Some researchers have used different conventional controlling technique for different combination of hybrid energy systems [40]. Natsheh et al [41] developed a novel model of smart grid-connected PV/WT hybrid system. It comprises photovoltaic array, wind turbine, asynchronous (induction) generator, controller and converters. The model was implemented using MATLAB/SIMULINK software package. Perturb and observe (P and O) algorithm was used for maximizing the generated power based on maximum power point tracker (MPPT) implementation. The dynamic behavior of the proposed model was examined under different operating conditions. Solar irradiance, temperature and wind speed data is gathered from a grid connected, 28.8kW solar power system located in central Manchester. Real-time measured parameters were used as inputs for the developed system. The problem of stability was reported to affect the performance and power quality of the system.

Another research by Yerra et al [42] proposes a hybrid energy conversion system combining photovoltaic and wind turbine as a small-scale alternative source of electrical energy where conventional generation is not practical. The hybrid system consists of photovoltaic panels, wind turbines and storage batteries. The wind and PV are used as main energy sources, while the battery was used as back-up energy source. Two individual DC-DC boost converters were used to control the power flow to the load. A simple and cost effective control with DC-DC converter was used for maximum power point tracking (MPPT) and hence maximum power was extracted from the turbine and the photo voltaic array. The modeling of hybrid system was developed in MATLAB- SIMULINK. Simulation results showed that the dynamic interaction between the load demand and the

renewable energy source caused critical problems of stability and power quality to the system.

Onur et al [43] designed proportional-integral (PI) controller and a fuzzy logic controller (FLC) that could fix the voltage amplitude to a constant value of 380 V and 50 Hz for loads supplied from a wind/battery hybrid energy system. The quality of the power produced by the wind turbine is affected by the continuous and unpredictable variations of the wind speed. Therefore, the voltage-stabilizing controllers was integrated into the system in order to keep the voltage magnitude and frequency constant at the load terminals, which requires constant voltage and frequency. A fuzzy logic-based controller was used for the voltage control of the designed hybrid system and compared with a classical PI controller for performance validation. The entire designed system was modeled and simulated using MATLAB/Simulink GUI (graphical user interface) with all of its subcomponents.

Beside the conventional approaches, some advanced control techniques exist, which can remove the power fluctuations caused by the variability of the renewable energy sources that may affect the quality of the power delivered to the load. In the literature, there are a few studies related to energy management of hybrid power system using advanced controlling techniques. Among them Syed Shah [44] developed an intelligent algorithms for a hybrid fuel Cell/photovoltaic standalone system. The developed system worked well and performed the expected function, the behavior of the FC and Battery to predict the upcoming events and perform the desired operations. These intelligent operations can save the fuel cost in the fuel cell and battery for the night consumption. The efficiency of the hybrid system increased by using a fuzzy based intelligent controller, and also helped to increase the operability of the hybrid system switching between Photovoltaic Cell (PC) and Fuel Cell (FC). Although the fuel cell increased the efficiency of the hybrid system, but one of the biggest disadvantages of fuel cells is

the cost to implement a system. Fueling fuel cells is still a major problem since the production, transportation, distribution and storage of hydrogen is difficult [44].

Francisco et al [45] developed a neural-fuzzy controller for a wind-diesel system composed of a stall regulated wind turbine with an induction generator connected to an a.c busbar in parallel with a diesel generator set having a synchronous generator. In their research, the gasifier was capable of converting tons of wood chips per day into a gaseous fuel that was fed into a diesel engine. The controller inputs were the engine speed error and its derivative for the governor part of the controller, and the voltage error and its derivative for the automatic voltage regulator. It was shown that by turning the fuzzy logic controllers, optimum time domain performance of autonomous a wind-diesel system could be achieved in a wide range of operating conditions compared to fixed parameters fuzzy logic controllers and PID controllers.

Dhanalakshmi and Palaniswami [46] carried out a research on the design and analysis of a Neuro-Fuzzy controller based on Adaptive Neuro-Fuzzy Inference System (ANFIS) architecture for Load frequency control of an isolated wind-micro hydro-diesel hybrid power system, to regulate the frequency and power deviations. They observed that, due to the sudden load changes and intermittent wind power, large frequency fluctuation problem could occur. Their developed control strategy combined the advantage of neural networks and fuzzy inference system and had simple structure that is easy to implement. So, in order to keep system performance near its optimum, it is desirable to track the operating conditions and use updated parameters to control the system. Simulations of the proposed ANFIS based Neuro-Fuzzy controller in an isolated wind-micro hydro-diesel hybrid power system with different load disturbances were performed. Also, a conventional proportional Integral (PI) controller and a fuzzy logic (FL) controller were designed separately to control the same hybrid power system for

the performance comparison. The performance of the proposed controller was verified from simulations and comparisons. Simulation results showed that the performance of the proposed ANFIS based Neuro-Fuzzy Controller could damp out the frequency deviation and attain the steady state value with less settling time.

Hee-Sang Ko and Kwang Y. Lee [47] proposed an intelligent adaptive system to control the output of a wind power generation plant to maintain the quality of electricity in the distribution system. The target wind generator was a cost-effective induction generator, while the plant was equipped with a small capacity energy storage based on conventional batteries, heater load for co-generation and braking, and a voltage smoothing device such as a static variable compensator (SVC). Fuzzy logic controller provided a flexible controller covering a wide range of energy/voltage compensation. A neural network inverse model was used to provide compensating control amount for a system. The system could optimized to cope with the fluctuating market-based electricity price conditions to lower the cost of electricity consumption or to maximize the power sales opportunities from the wind generation plant.

2.9 Summary of Research Gaps

Conventional approach for controlling power supply to the load requirement according to the demand was used in various hybrid systems [44]. However, the approaches still face the problem of stability and power quality that are not very common in conventional power systems using non renewable energy.For stand-alone PV-Wind hybrid power system, lead-acid batteries play a vital role as an energy storage unit. Even though batteries are the weaker section in the overall system, they are in need of certain initial investment of equipment. As the management of charging/discharging in storage battery directly affects the qual-

ity of power supply in the hybrid system since electric energy from wind turbine generator and solar cells has obvious fluctuation. It makes the system great demand to electric power management. Therefore, it is significant to study power management of the hybrid system in detail. Conventional control theories do not have good performance for the hybrid power system,Literature shows that using artificial intelligence techniques can remove the power fluctuations caused by the variability of the renewable energy sources that may affect the quality of the power delivered to the load. The focus of this research is to design an intelligent controller which is capable of optimizing the power generated by renewable energy sources. The research also introduces a new control strategy for power flow in stand-alone pv-wind hybrid power systems based on fuzzy logic. The proposed controller manages the power flow between three energy sources comprising of PV panels, wind turbine and battery storage. The overall aim is to optimize the active power flow between system power sources for different modes of operation, and to maintain the battery state-of-charge (SOC) at a reasonable level.

CHAPTER THREE
DEVELOPMENT OF PV-WIND HYBRID POWER SYSTEM MODEL

In power applications and system design, modeling and simulation are essential to optimize control and enhance system operations. In this chapter, the models for the main components of the proposed hybrid power system are developed and validated. It includes photovoltaic power system, wind turbine power system, battery storage, dc-dc converter and dc-ac converter. In addition, the MATLAB Simulink circuit block models for each system are shown in respective section.

3.1 System Description

Modeling of the PV-Wind hybrid system is carried out using MATLAB Simulink. The Solar-Wind Hybrid Power System (SWHPS) consists of several units, PV power and wind power units as primary sources of energy, battery bank unit as auxiliary source of energy, dc-dc and dc-ac converters, load unit and control unit. The function of controller unit is to ensure the management of the power, which is delivered by the hybrid system to satisfy the load demand and to charge the battery. The function of dc-dc converter is to convert the unregulated DC voltage to produce regulated voltage. The inverter unit is used to convert the DC generated power from renewable energy sources to feed the load with the required AC power. The excessive charge from the battery will be dumped to the dump load unit. The dump load in this case is the battery storage which can then be used to supply power to the load in case of insufficient power generated by primary sources. Blocks such as wind model, photovoltaic model, dc-dc converter model, dc-ac converter model and the energy storage model are built separately before combining into a complete hybrid system. The block diagram describing the

system conceptual framework is shown in Figure 4.1. The mathematical models describing the dynamic behavior of each of these components are discussed in next section.

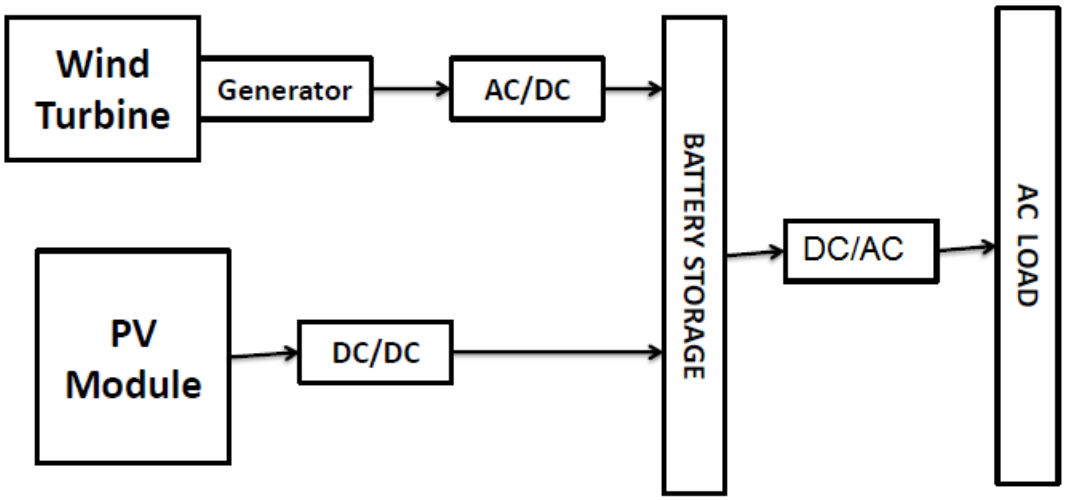

Figure 3.1: Block diagram of system conceptual framework

3.2 Modeling of Wind Turbine

The wind turbine power system consists of a wind turbine model and a Permanent Magnet Synchronous Machine (PMSM) block that is available in the Simulink library. The model of wind turbine is developed based on its steady-state characteristics, as stated in Equations (2.6) to (2.13). Included inside the model was a subsystem that was used to determine the power coefficient $Cp(\lambda, \beta)$ value when tip speed ratio (λ) and blade pitch angle β change. This uncontrolled model is used to represent the wind turbine without application of the maximum power point tracker. Figure 3.2 shows the wind turbine block model generated by Simulink. This model is used as a foundation for later models incorporating the FLC, and its purpose is to optimize the power generated by the wind turbine.

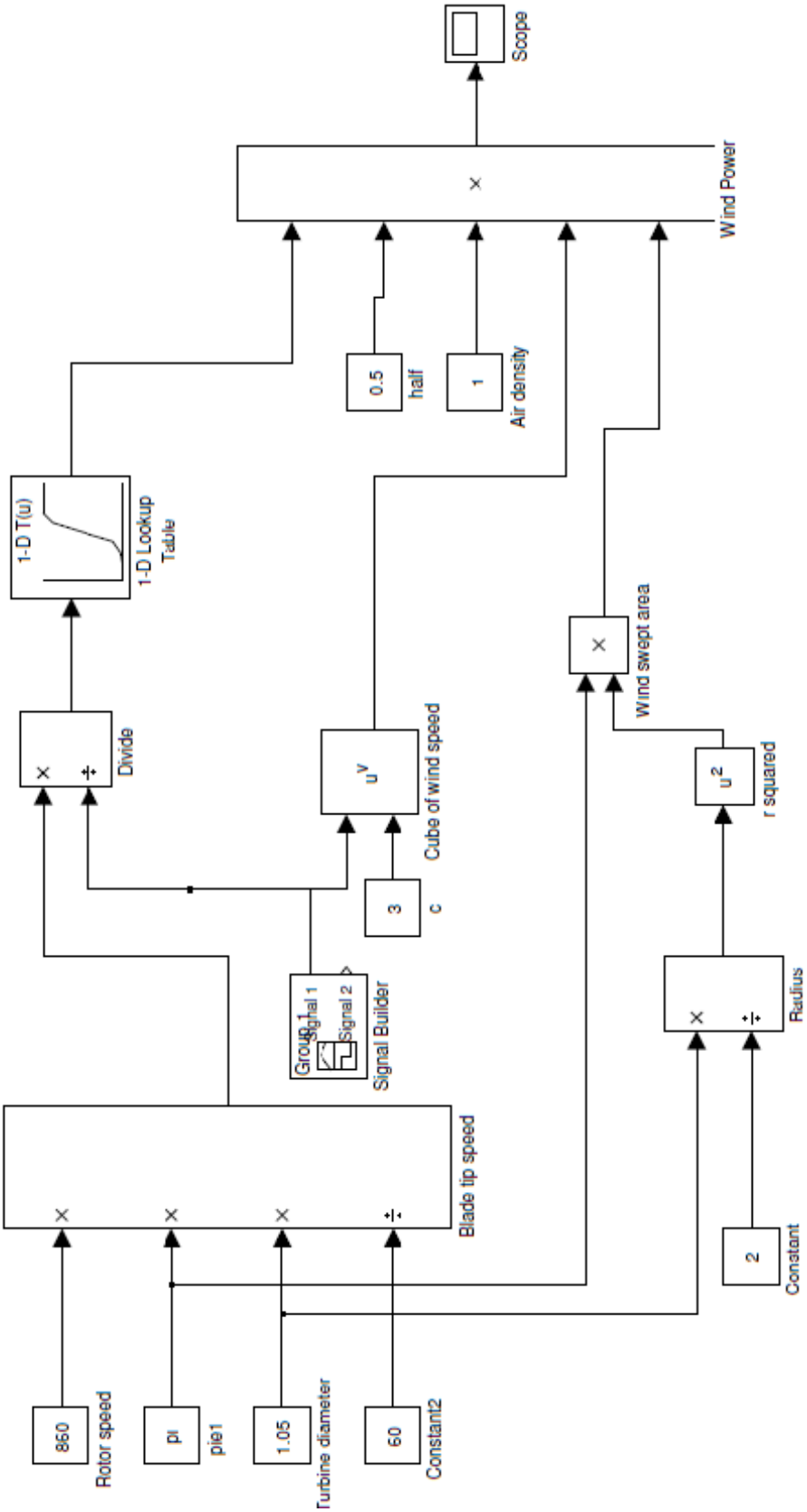

Figure 3.2: Wind turbine block model generated by Simulink

3.3 Modeling of Photovoltaic Module

The PV system model was developed based on Equations (2.1), (2.2),(2.3) and (2.4). Parameters such as the open-circuit voltage (Voc), the short-circuit current (Isc), the maximum power point voltage ($Vmpp$), the maximum power current ($Impp$) and the temperature coefficient (Kv) were obtained from the data sheet of the selected PV module.

In this Research, Apollo 100-18-P photovoltaic module was chosen as reference to develop the PV block model. The electrical specifications for Apollo 100-18-P are shown in Table 3.1.

Table 3.1: Electrical Specifications of Apollo 100-18-P PV Module

Parameter	Variable	Value
Rated Maximum Power	$Pmax$	100W
Voltage at $Pmax$	Vmp	18.66V
Current at $Pmax$	Imp	5.36A
Open Circuit Voltage	Voc	22.72V
Short Circuit Current	Isc	5.34A
Nominal operating cell temperature	NOCT	47 ± 2°C
Operating Temperature	OT	-40°C to 65°C

The proposed PV model was generated and simulated using Matlab-Simulink. Figure 3.3 shows the resulting Matlab-simulink model.

Both P-V and I-V output characteristics of the generalized PV model are shown as simulated using Figures 3.4 and 3.5. The nonlinear nature of PV module is apparent as shown in the figures, i.e., the output power and current of PV module depend on the solar irradiance and cell temperature, and the cell terminal

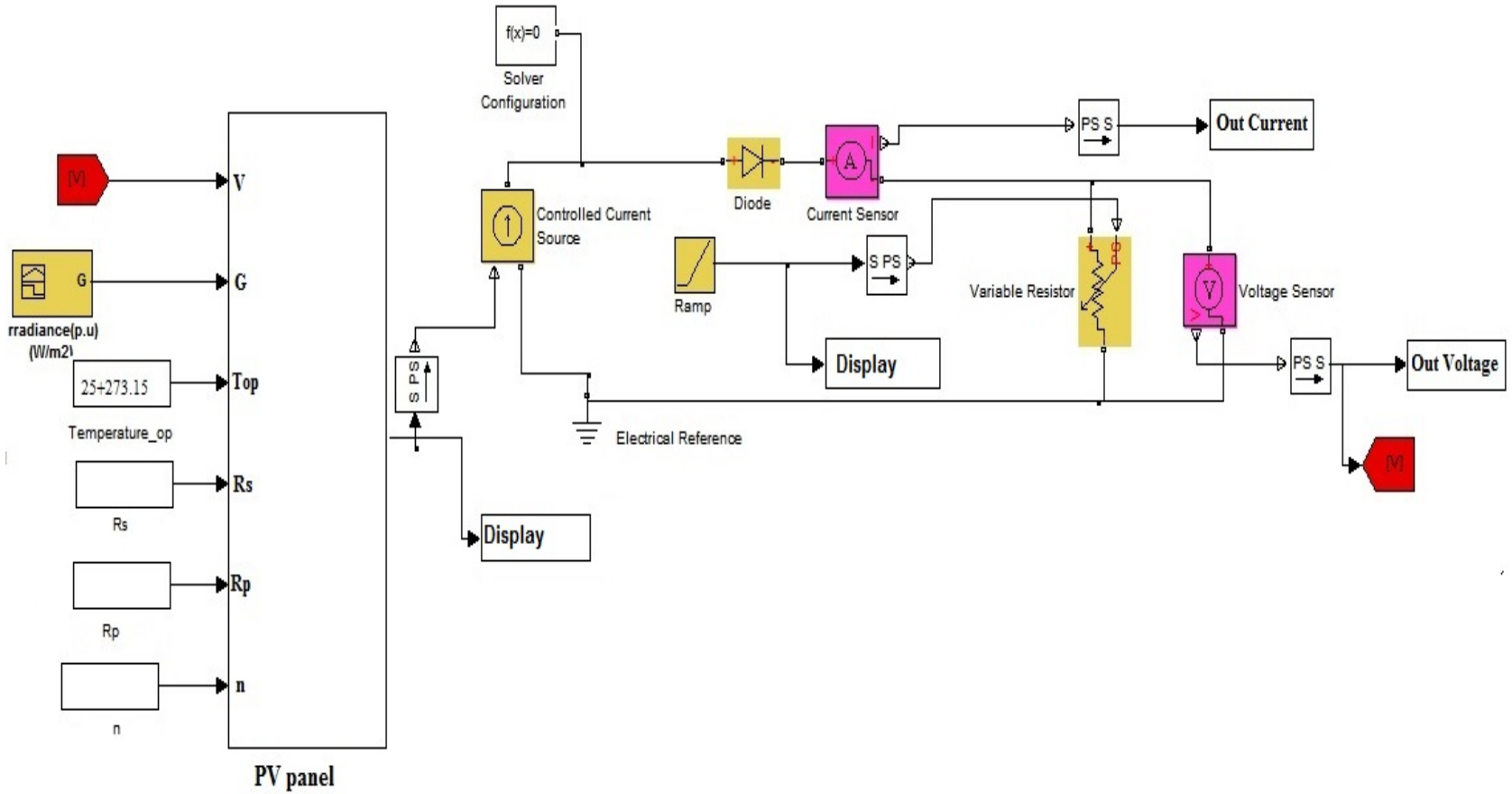

Figure 3.3: PV model generated by Simulink

operating voltage as well. It can be seen from Figure 3.4 that, with increased solar irradiance, there is an increase in both the maximum power output and the short circuit current. On the other hand, Figure 3.5 shows that with an increase in the cell temperature, the maximum power output decreases whilst the short circuit current increases.

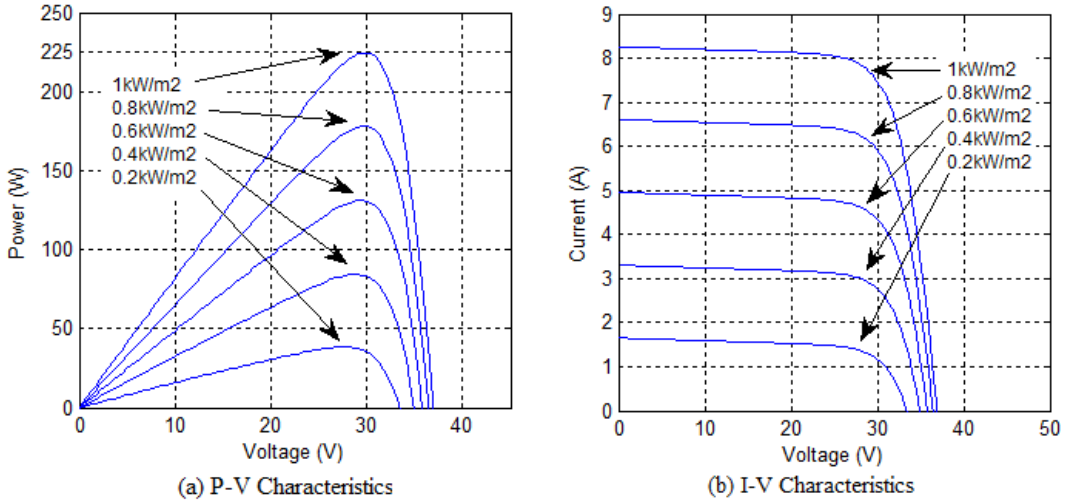

Figure 3.4: I-V and P-V output characteristics with different Irradiance

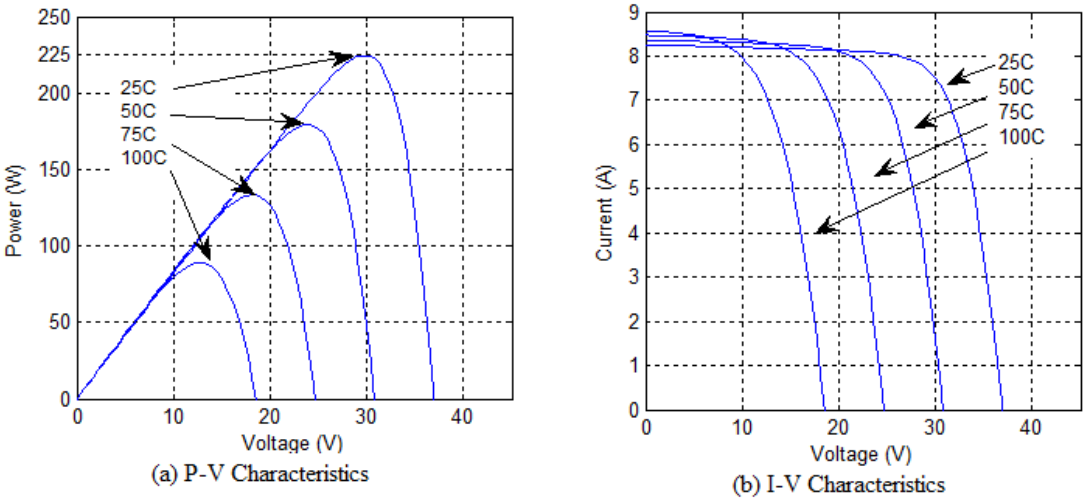

Figure 3.5: I-V and P-V output characteristics with different Temperature

Modeling of Battery Storage

A validated electrical circuit model for lead-acid batteries, shown in Figure 3.6 is available in Matlab-Simulink library, as reported in [48] .

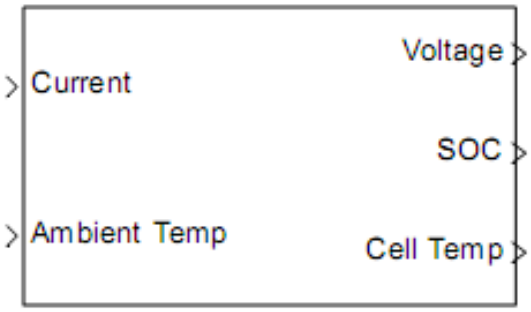

Figure 3.6: Battery Model

The battery model was designed to accept inputs for current and ambient temperature, as shown in Figure 3.6. The outputs were voltage, SOC, and electrolyte temperature. A diagram of the overall battery model structure is shown in Figure 3.7, which contains three major parts: a thermal model, a charge and capacity model, and an equivalent circuit model. The thermal model tracks electrolyte temperature and depends on thermal properties and losses in the battery. The charge and capacity model tracks the battery's state of charge (SOC), depth of charge remaining with respect to discharge current (DOC), and the battery's capacity. The charge and capacity model depends on temperature and discharge current. The battery circuit equations model simulates a battery equivalent circuit. The equivalent circuit depends on battery current and several nonlinear circuit elements [48]

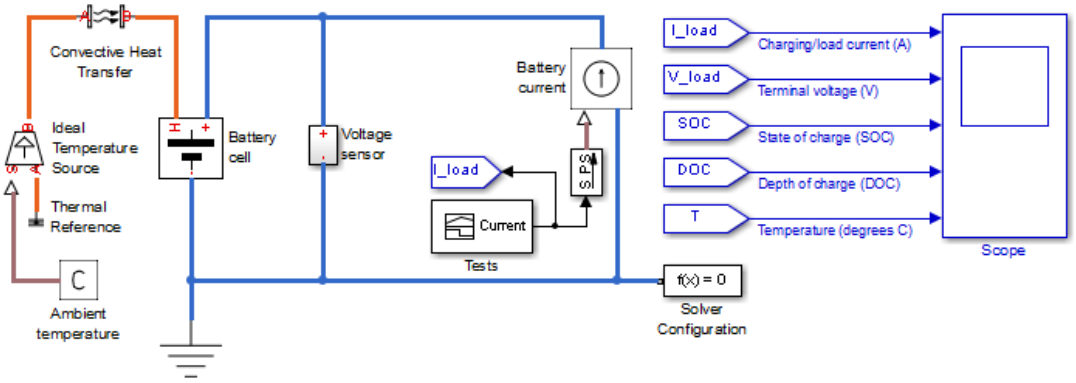

Figure 3.7: Battery model generated by Simulink

Modeling of DC-DC Converter

To connect a photovoltaic or wind turbine to an external power system (e.g. DC load), it is necessary to boost their voltage. Therefore, a DC averaged switched model converter is needed to regulate the output voltage before being supplied to other electronic devices. There are many DC-DC converters including the step-down (buck) converter, the step-up (boost) converter, the buck-boost converter and many others The model describing DC-DC converter is available in Simulink library. In order to simulate the converters, the equations that describe the converter operation on each of the three possible operating stages are implemented in Matlab, and solved using Matlab facilities. The program structure consists in two files. The first file initializes the default values of converter parameters, that is, the input voltage E, the inductance value L, the capacitor value C, the load value R, the switching period T, the duty-cycle D and the number of periods to be displayed. All the parameters can be changed during the converter simulation. The second file solves the differential equations that describe the converter operation and calculate the critical values of inductor for continuous conduction mode operation and value of output voltage. Also, define the plots for output voltage and input current. This model can be readily used for any closed loop design, that is, PI or fuzzy. Figure 3.8 shows a Simulink model for a closed loop

dc-dc converter.

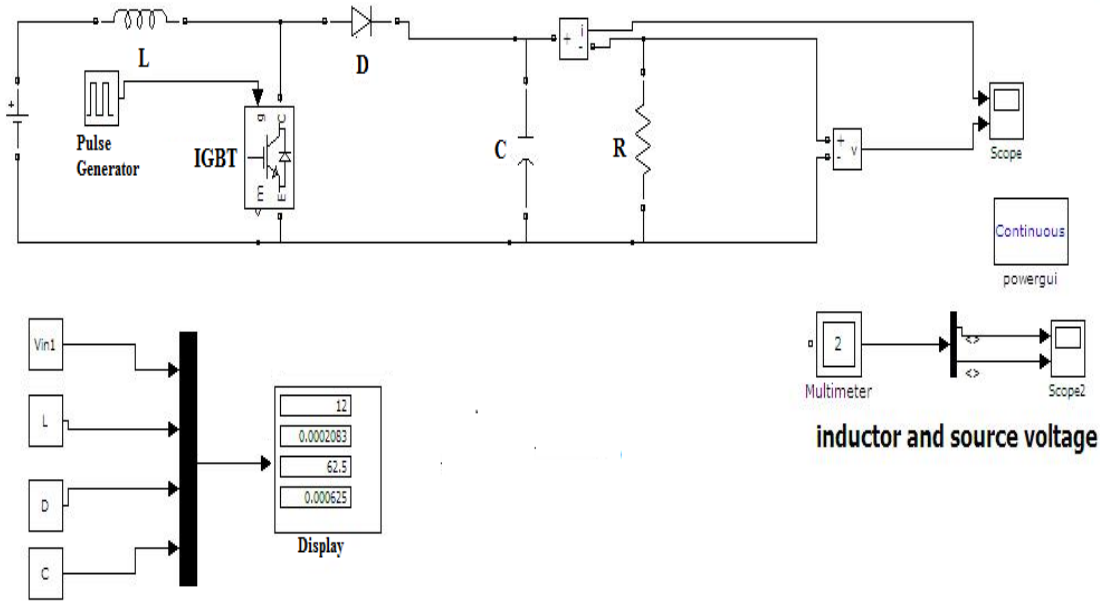

Figure 3.8: Simulink model for a dc-dc converter

Modeling of DC-AC Converter

DC-AC inverters are electronic devices used to produce mains voltage AC power from low voltage DC energy (from a battery or solar panel). This makes them very suitable when you need to use AC power tools or appliances. The model describing the operation of inverter is implemented in the Simulink block as shown in Figure 3.9. It was developed using a universal bridge IGBT.

Overall PV-Wind hybrid power system model

After completing the standalone system modeling for PV model, wind model, battery model and dc-dc converter model, all individual models were connected as hybrid system. AC voltage generated by wind model was rectified and converted into DC voltage. It is then added with DC voltage from PV model and then connected to battery and the load. The schematic of the overall PV-Wind hybrid

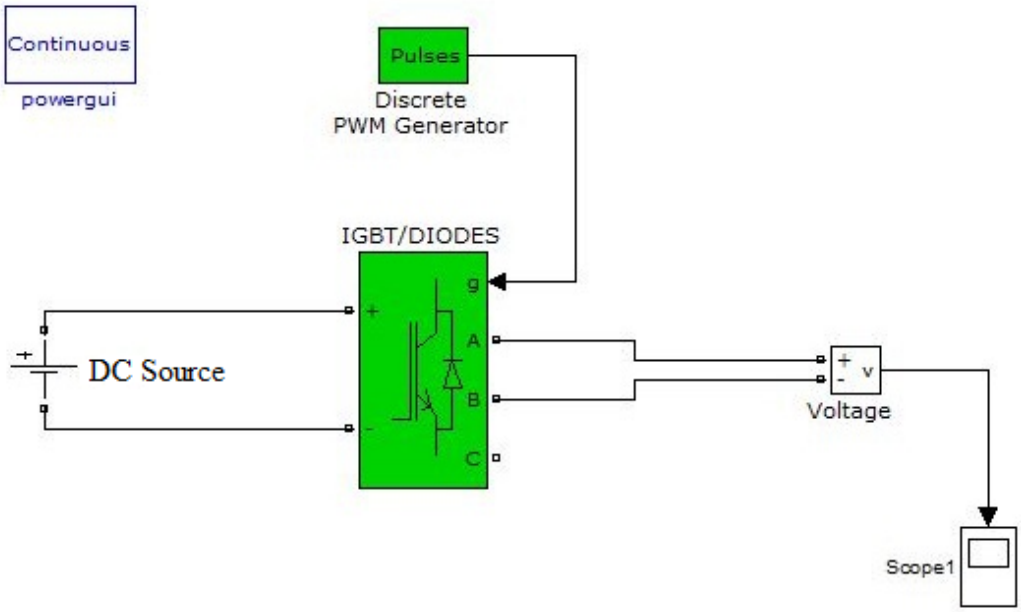

Figure 3.9: Simulink model for a dc-ac converter

power system model is shown in Figure 3.10.

System Model validation

All individual models were validated separately before combining to form the hybrid system. The battery mode and dc-dc and dc-ac converters are adapted from the Simulink built-in SimPowerSystem. This study also adopt the wind turbine model developed and validated by Lina [49]. Figure 3.11 shows the wind turbine power characteristics of the validated model. The PV model was validated through a series of experiments. Figure 3.12. shows the experimental setup.

The experimental setup consists of Apollo 100-18-P solar panel, adjustable load resistance, and some measurement instrumentation. The PV module was placed at an inclination angle of 45° . A series of measurements were then conducted using the set up on a sunny day (1000W/m^2). Measurements were taken under different load settings, as shown in Table 3.2 (sample selected data). Observa-

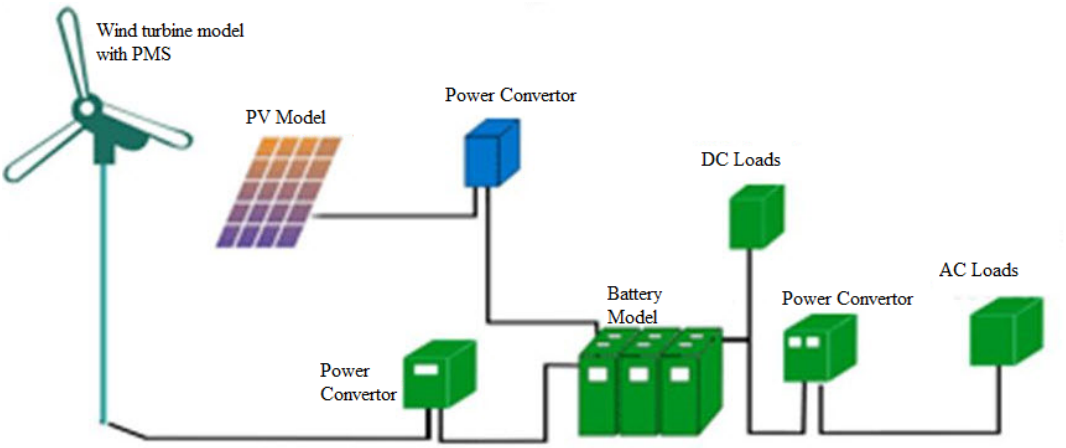

Figure 3.10: Schematic of overall PV-Wind hybrid power system model

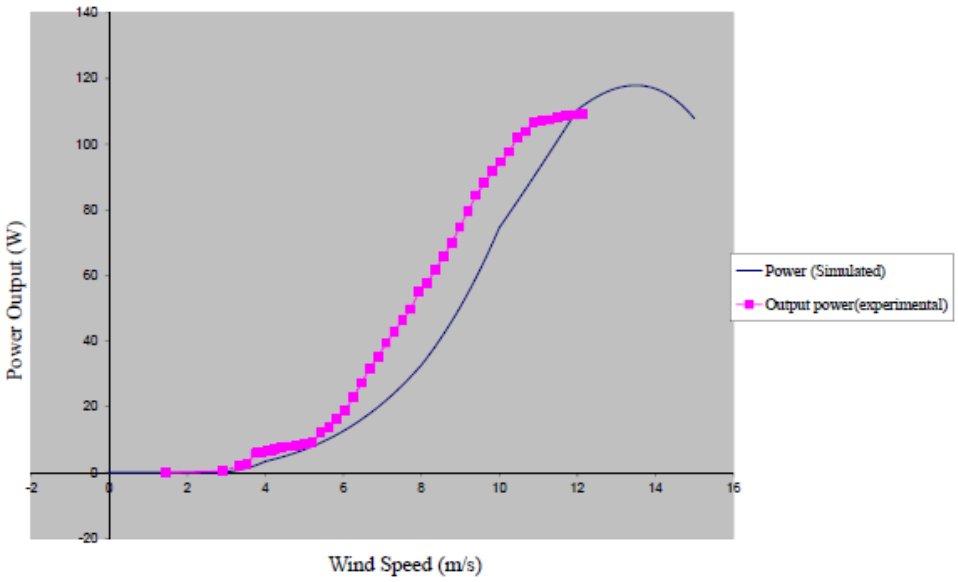

Figure 3.11: Wind turbine power characteristics

tions of temperature, solar irradiance, working voltage and output current of PV module were taken and recorded each time the load was changed. It was found that both simulated and measured results for the output power of PV module are in good agreement, the difference was observed to be less than 2%. It was concluded that the model provides sufficient accuracy for simulations.

The model is used as a foundation for later models incorporating the ANFIS, and its purpose is to optimize the power generated by the photovoltaic system.

Figure 3.12: Experimental setup for the PV model validation

Table 3.2: Experiment results for the Apollo 100-18-P solar panel

Load (Ω)	Voltave (V)	Current (A)	Power (W)
1	8.30	8.16	67.73
2	16.11	8.17	131.62
3	24.35	8.11	197.48
4	29.89	7.41	221.48
5	32.44	6.47	209.89
6	33.52	5.69	190.73
7	34.58	4.70	162.53
8	34.94	3.91	135.21
9	35.1	3.26	114.43
10	35.4	2.81	99.47

CHAPTER FOUR
DEVELOPMENT OF OPTIMAL POWER MANAGEMENT ALGORITHM

4.1 Introduction

This Chapter presents an optimized management strategy for power flow in stand-alone PV-Wind hybrid power systems. The method offers on-line energy management by a hierarchical controller between three energy sources comprising of photovoltaic panels, wind turbine and battery storage. The proposed method includes a MPPT controller in the first layer, to achieve the maximum power point (MPP) of PV panels; two different techniques will be presented (P&O and neural network). P & O is used for comparison purposes. In the second stage, Fuzzy logic controller will be developed to distribute the power among the hybrid system and to manage the charge and discharge current flow for performance optimization. Finally, in the third layer an FLC Controller is developed to achieve the MPP of the Wind turbine. Figure 4.1 shows the proposed control structure for the hybrid system. The structure of FLC and ANN are attached in Appendices A and B.

4.2 Perturb and Observe PV Maximum Power Point Tracking Algorithm

The problem considered by MPPT techniques is to automatically find the optimum voltage ($VMPP$) or current ($IMPP$) at which a PV module should operate, under a given solar irradiance and temperature. Perturb and observe method is the most commonly used technique because of its simplicity and ease of implementation [15]. It requires two inputs; measurement of the current (Ipv) and

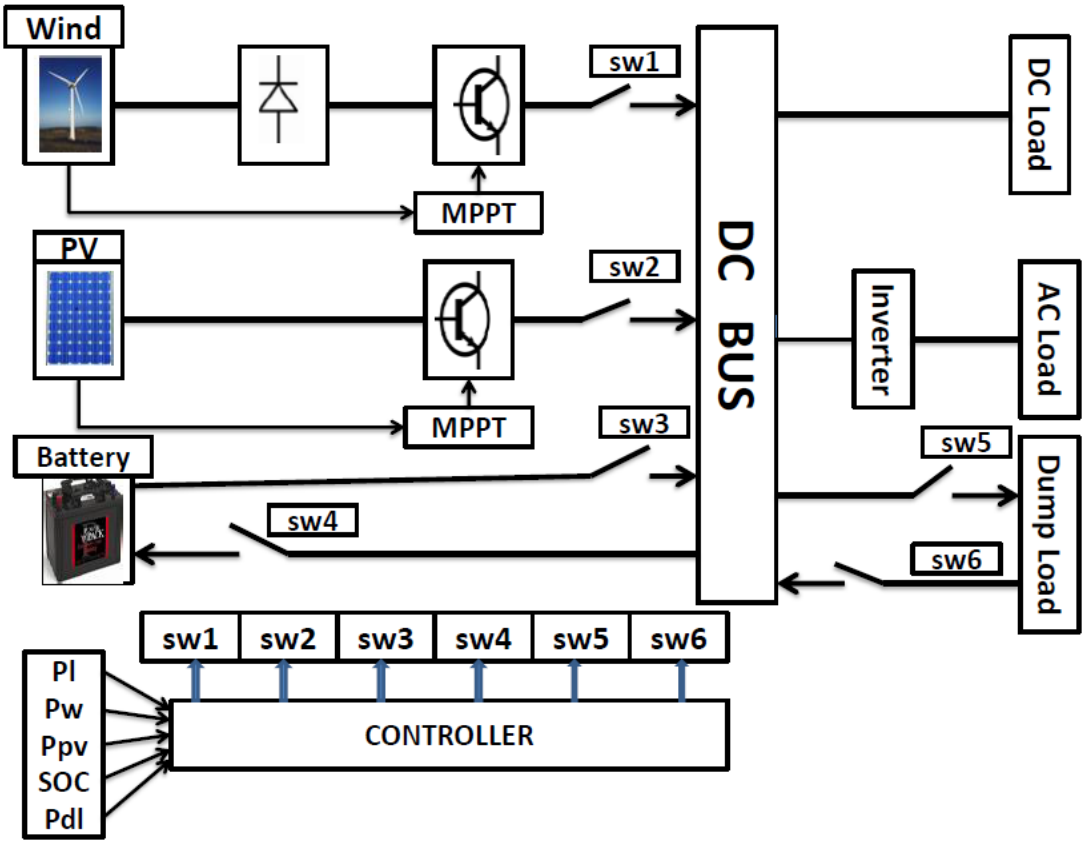

Figure 4.1: Block diagram of the proposed system

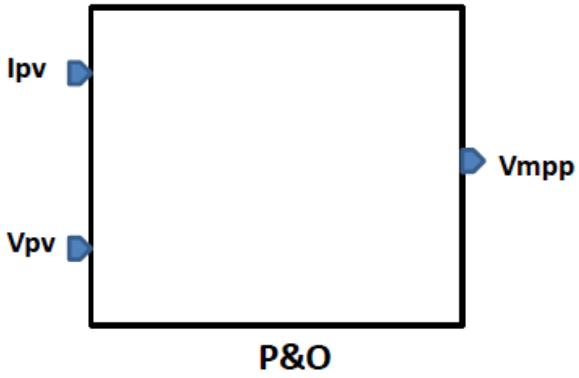

Figure 4.2: P&O block diagram

measurement of the voltage (Vpv) as shown in Figure 4.2.

The P&O algorithm operates by periodically perturbing (incrementing or decrementing) the PV array terminal voltage or current, and comparing the PV output

power with the previous one. If it is positive, the control system moves the PV array operating point in the same direction; otherwise, it is moved in the opposite direction. In the next perturbation cycle, the algorithm continues in the same way. Figure 4.3 shows the flow chart of P&O algorithm. The main problem of this method can be seen when solar radiation rapidly changes. As illustrated in Figure 4.4, starting from an operating point A, if atmospheric conditions stay approximately constant, the voltage perturbation (ΔV) will bring the operating point to B and the perturbation will be reversed due to a decrease in power. On the other hand, if the irradiance increases and shifts the power curve from $P1$ to $P2$ within one sampling period, the operating point will move from A to C (this represents an increase in the power and the perturbation is kept the same). Consequently, the operating point diverges from the MPP and will keep diverging if the irradiance steadily increases [18].

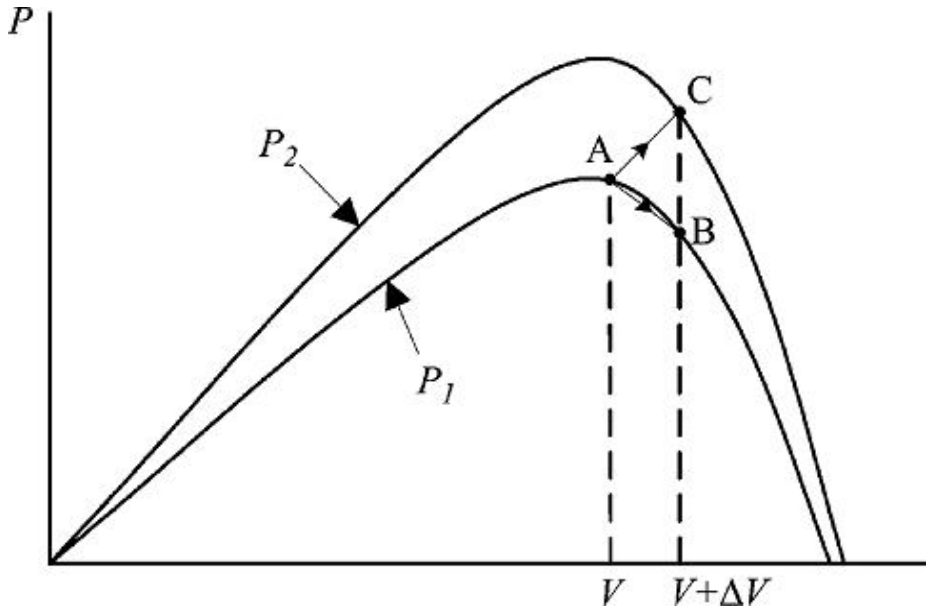

Figure 4.4: Divergence of P&O from MPP

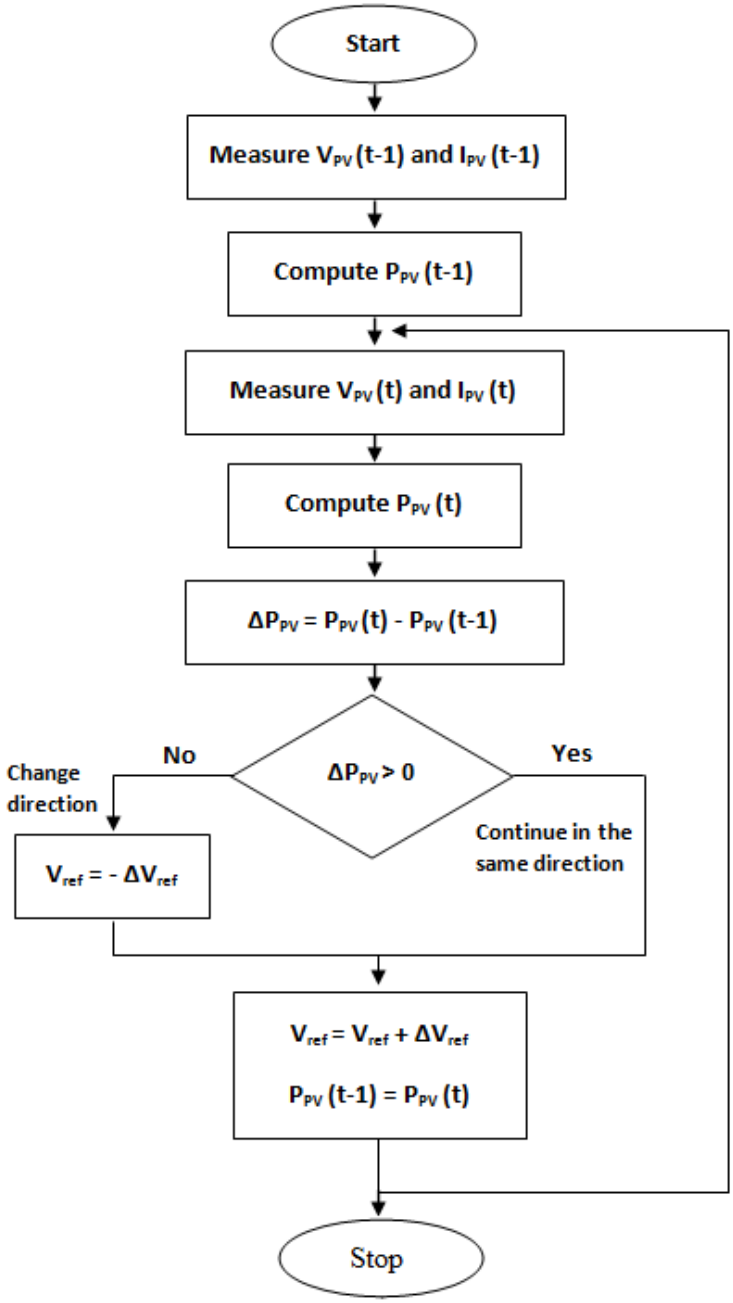

Figure 4.3: P&O algorithm flow chart

4.3 ANFIS Based PV Maximum Power Point Tracking

The ANN was trained to recognize the relationships between the input and output parameters. The developed PV model is used to collect the training data comprising of solar irradiance, temperature and output voltage which is then used to train the network to obtain the inputs of the FLC. The operating temperature is varied from 15° C to 65° C in steps of 5°C and the solar irradiance level is varied from 100 W/m^2 to 1000 W/m^2 in steps of 50 W/m^2, to get the training data sets for ANFIS. For each pair of operating temperature and irradiance level the reference voltage corresponding to the maximum available power is recorded. Figure 4.5 shows the proposed ANFIS based PV MPPT controller.

The ANFIS controller design involves the following steps;

1. Identification of the inputs, outputs and their ranges.
2. Design of the fuzzy membership functions for each input and output by the use of ANFIS.

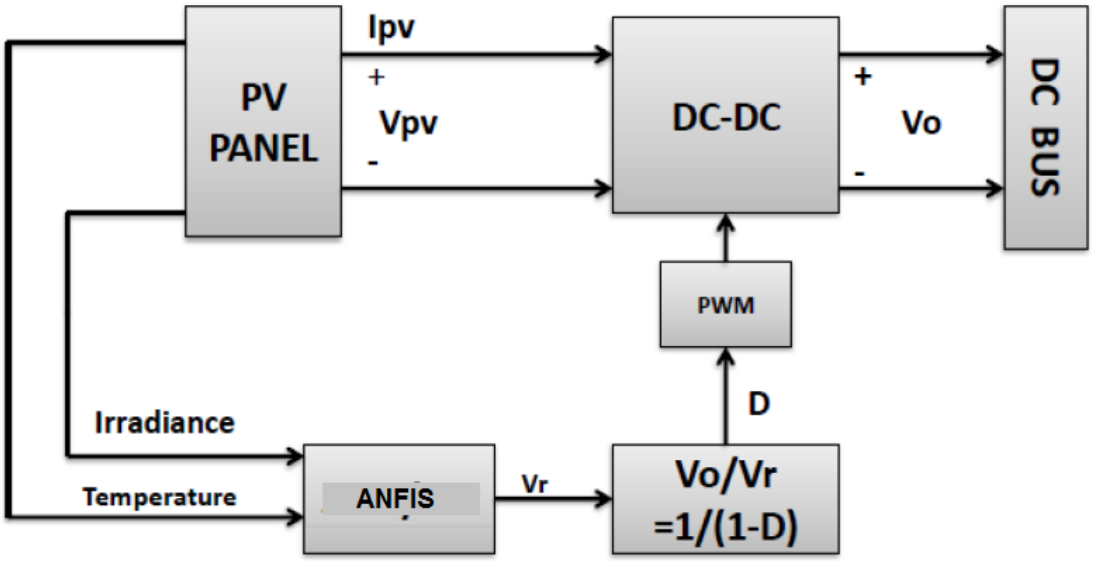

Figure 4.5: The proposed ANFIS based PV MPPT controller

3. Construction of the knowledge base that contains the fuzzy rules which are used for fuzzy reasoning. The knowledge base is constructed by ANFIS.

4. Mapping of the fuzzy logic controller's output to the corresponding crisp values by use of center of gravity defuzzification procedure.

Identification of the Inputs, Outputs and their Ranges.

The neural network controller (NNC) is used to estimate the PV array operating voltage (Vref), which corresponds to Pmax at any given solar radiation and cell temperature. Therefore the inputs to the controller are the solar radiation and the cell temperature. The output of the controller is the optimum operating voltage.

Design of Membership Functions and the Rule Base

The design of membership functions is achieved by use of ANFIS as follows:

1. A set of training data which corresponds to the maximum power (Pmax) at any given solar radiation and cell temperature is presented to the ANFIS. This set of data is generated from the developed PV model discussed in section 3.2.2. Typical example of training data set are shown in Table 3.3

2. The ANFIS is generated by use of grid partitioning, which is a method for grouping data into clusters based on their similarity. The ANFIS is then trained by use of hybrid learning rule. The hybrid learning rule combines the gradient method and the least squares estimation (LSE).

3. Different sets of data are presented to the ANFIS, and based on the input-output relationship of the ANFIS, the membership functions for the FLC are constructed.

4. The rule base for the FLC is generated based on the execution of the ANFIS. This is because, ANFIS automatically generates its own rule base depending on its set of training data. In this case 203 sets of training data were gathered through simulation (Appendix C). Table 4.1 shows typical examples of training data sets when irradiance varies and temperature is kept constant.

Table 4.1: Typical examples of the training data set.

Irradiance	Temperature	Voltage (V)
100	15	21.22
150	15	21.69
200	15	22.00
250	15	22.21
300	15	22.37
350	15	22.49
400	15	22.58
450	15	22.65
500	15	22.71
550	15	22.74
600	15	22.77
650	15	22.79
700	15	22.80
750	15	22.80
800	15	22.80
850	15	22.79
900	15	22.78
950	15	22.76
950	15	22.74

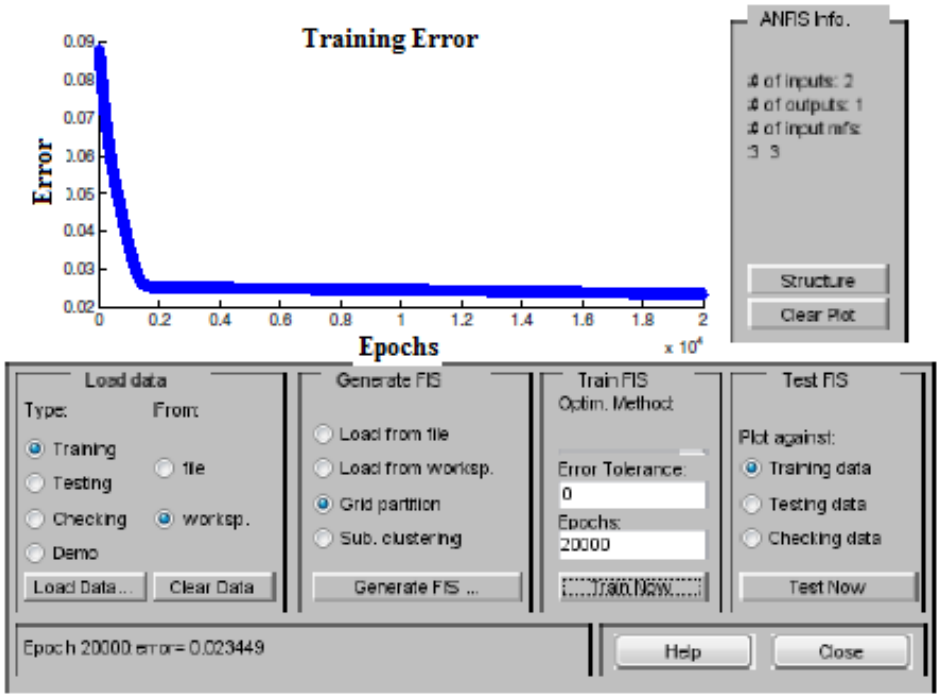

Figure 4.6: A screen shot of the ANFIS editor for the PV Model

The ANFIS that is used in the tuning of fuzzy membership functions is explained using Figures 4.6 through 4.10. The proposed ANFIS uses Sugeno inference mechanism. The main reason for the use of Sugeno inference mechanism is the ability of the inference mechanism to model non-linear problems. In this type of inference mechanism, the output is a function of the inputs and is a fuzzy singleton. Figure 4.6 is a screen shot of the ANFIS editor. It shows a plot of the training error after the training process. As is shown in Figure, the ANFIS is generated with grid partitioning fuzzy inference mechanism, where each input is assigned three membership functions, and then trained with 20,000 epochs (number of iterations for training) using hybrid learning rule. Figure 4.7 shows the block representation of the ANFIS which uses Sugeno inference system. Figure 4.8 shows the structure of the ANFIS and the parameters used in its execution process. In Figure 4.8, 'input' represents the inputs which are solar irradiance and cell temperature and 'inputmf' represents the input membership functions; 'rule' represents the rules,'outputmf' represents the output membership functions

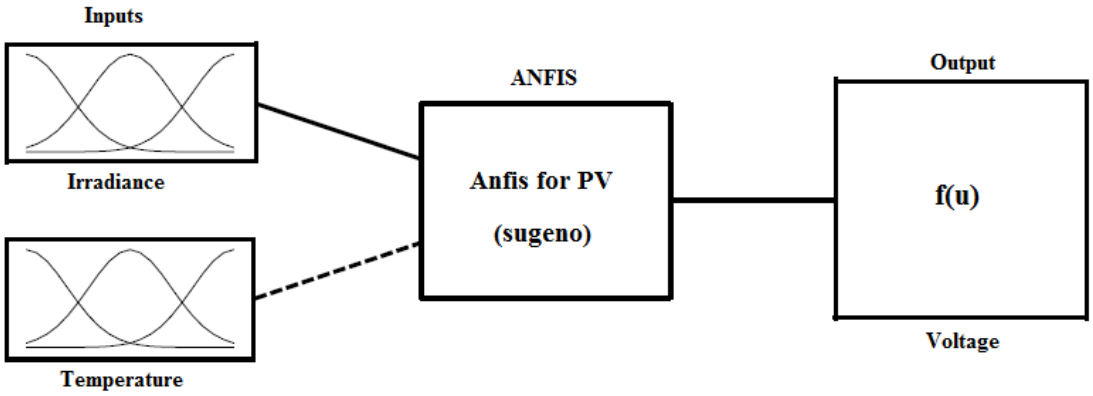

Figure 4.7: A Block representation of the ANFIS

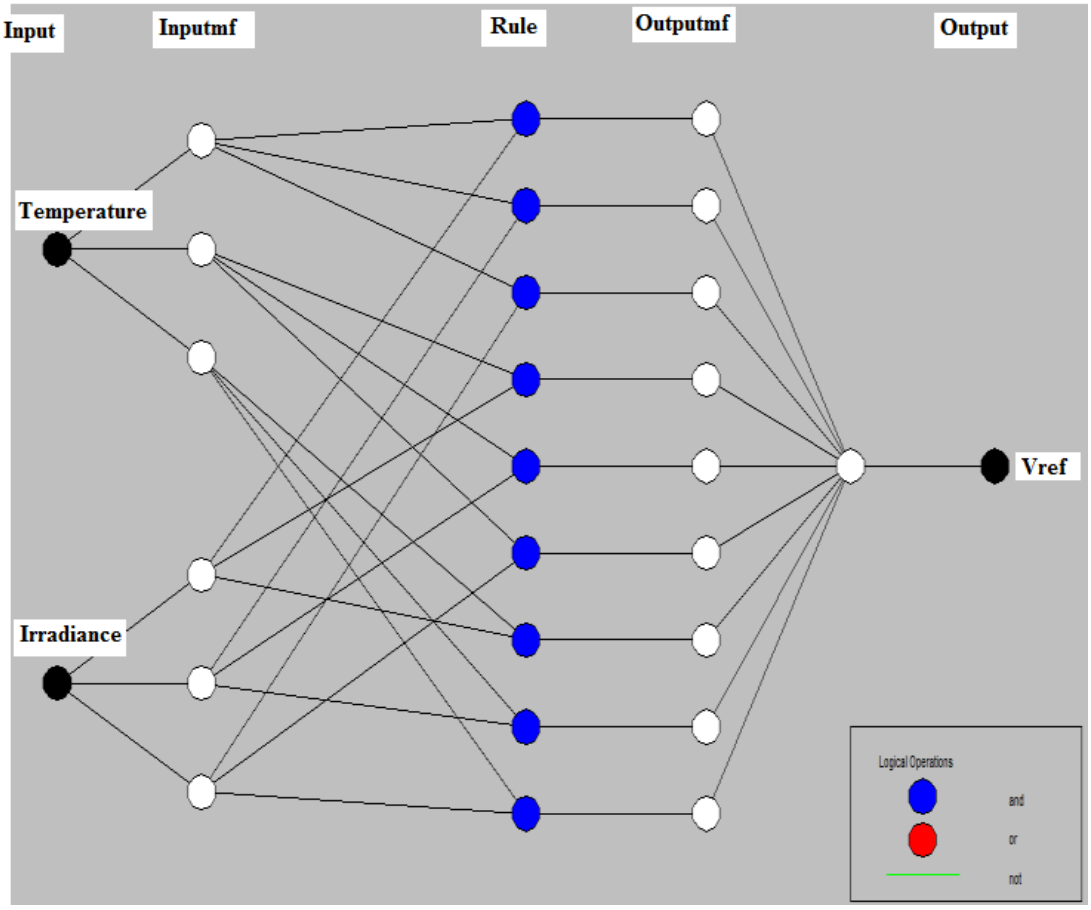

Figure 4.8: Structure of the ANFIS

and 'output' represents the output. Figure 4.9 represents membership functions for the two inputs, namely, irradiance and Temperature. Figure 4.10 shows a screen shot of diagrammatic representation of some of the rules for the ANFIS.

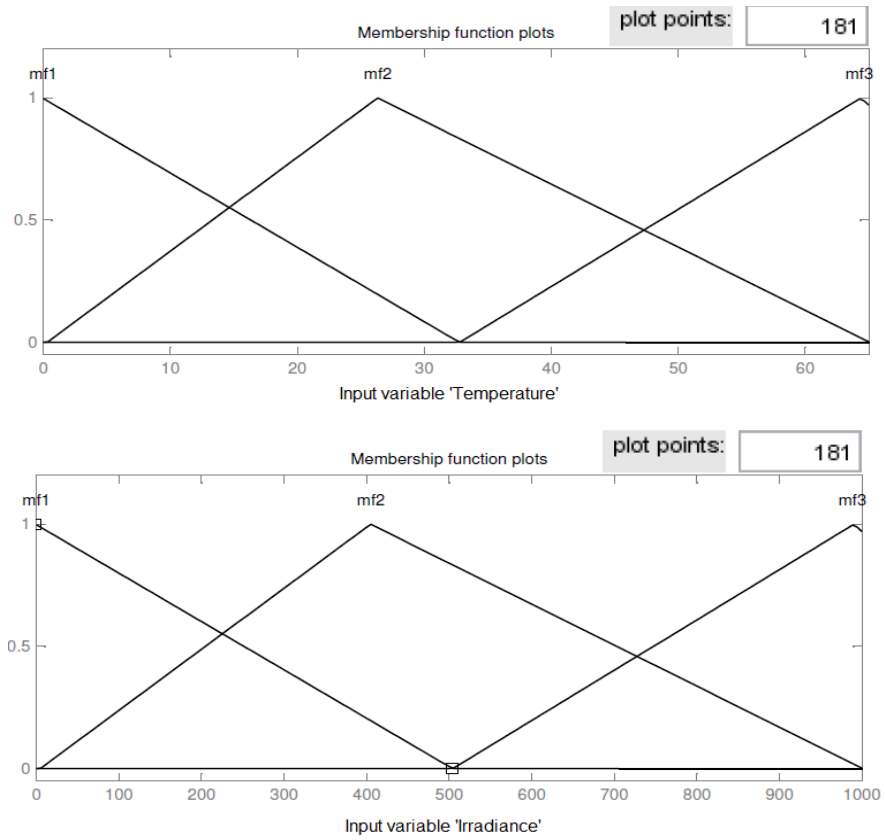

Figure 4.9: Membership functions of the inputs

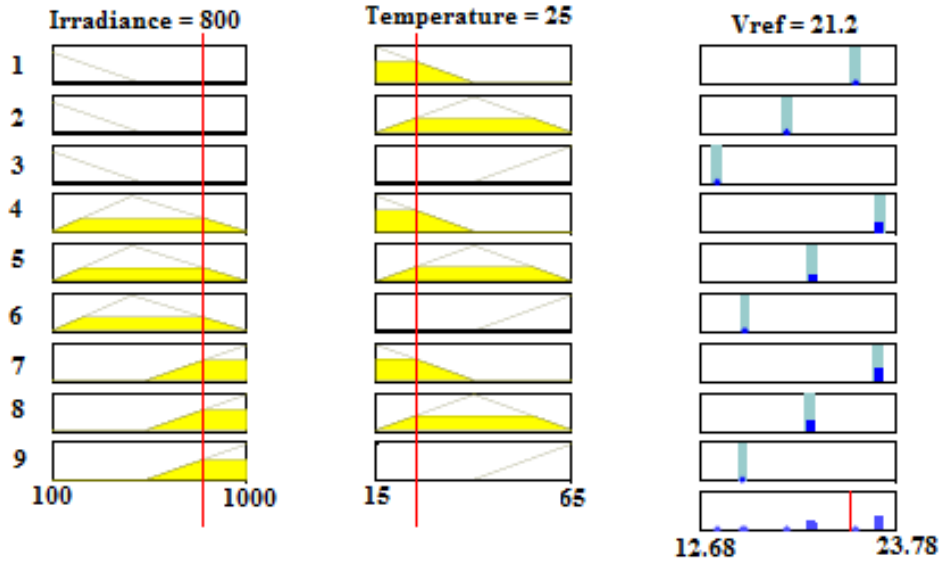

Figure 4.10: Screen shot of diagrammatic representation of some of the rules for the ANFIS

Implementation of ANFIS Based PV MPPT

Figure 4.11 shows the block diagram for the proposed controller which was implemented in MATLAB/Simulink. The simulation results and discussion are presented in chapter 5.

4.4 FLC Based Wind Maximum Power Point Tracking

Figure 4.12 presents the block diagram of the wind energy conversion system adopted in this research; wind energy by wind turbines is converted into mechanical power on the shaft. Mechanical power is converted into electrical power by a permanent magnet synchronous generator (PMSG). The generator AC output voltage is converted to dc form using a full-wave bridge rectifier. The boost DC-DC converter to control the output voltage of the rectifier (Vdc) is used. Rectifier output voltage and current are measured and sent to the controller. In this research, the fuzzy algorithm is used to achieve the maximum power point. In this methodology, the load voltage and current measurements and output power are calculated and sent to the controller. Figure 4.13 show the block diagram of the controller used in this case. During the control process, fuzzy membership functions with a range of 0 and 1 are used to convert the controller's input variables to membership values. For the FLC used, membership functions are chosen to be of triangular form for reasons of simplicity since they are less demanding in computational resources. Two inputs for the FLC are the output power variation, ΔPn and the converter's output duty cycle difference, $\Delta Dn - 1$.

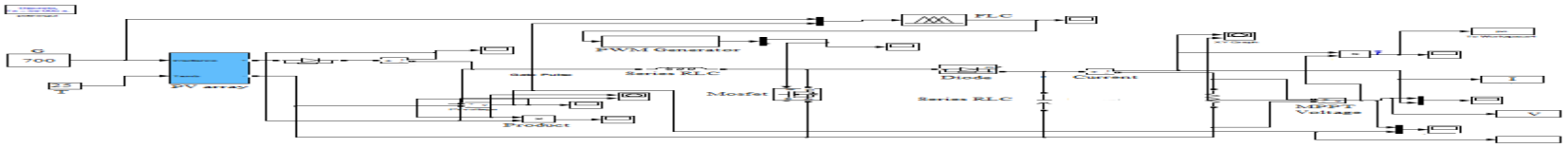

Figure 4.11: PV MPPT model generated by Simulink

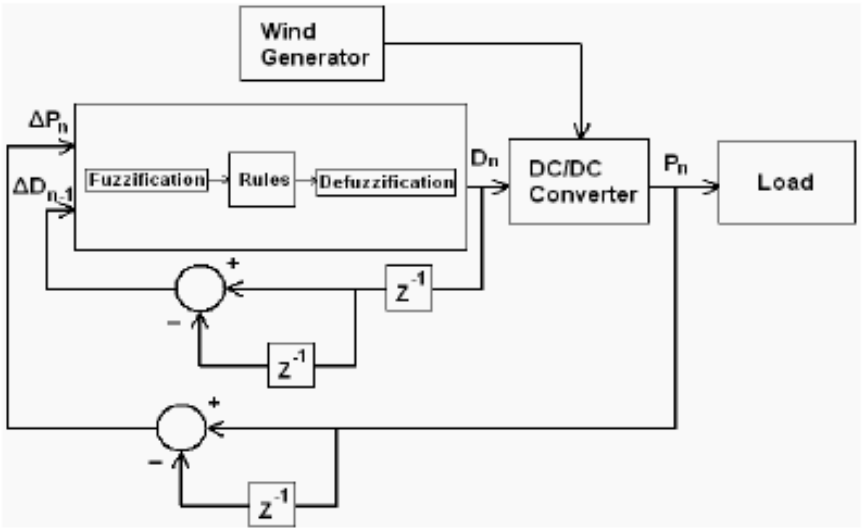

Figure 4.13: Block diagram of the FLC based wind MPPT

$$\Delta Pn = Pn - P(n-1) \tag{4.1}$$

$$\Delta D_n^i = D_{n-1}^\circ - D_{n-2}^\circ \tag{4.2}$$

For the fuzzy inference engine, "IF-THEN" rules with "AND" logical operators are designed. Table 4.2 displays the rules governing the controller's operation. Fuzzy variables negative large (nl),negative medium (nm), negative small (ns), zero (z),positive small (ps),Positive medium (pm) and positive large (pl) are used for inputs wheres fuzzy variable very large (vl), medium large (ml), above average

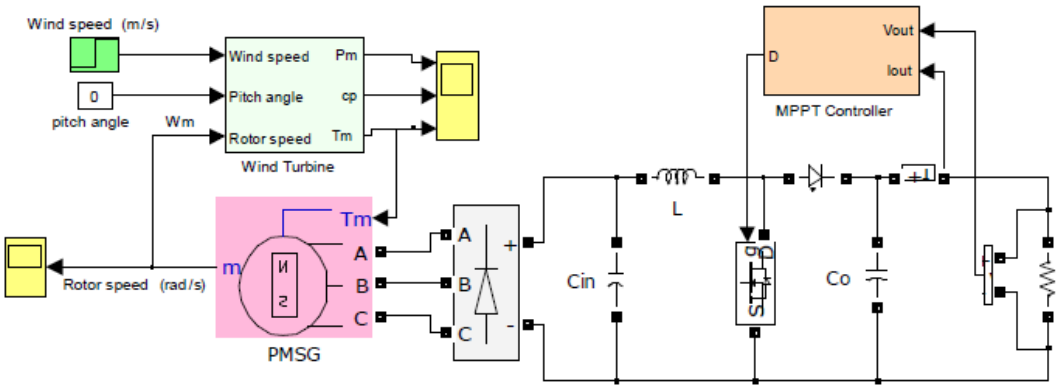

Figure 4.12: Block diagram of the wind energy conversion system

(aav), average (av), below average (bav),medium small (ms) and very small are used for outputs. The system measures the output power difference ΔPn and adjusts D in order to track the MPP. Figure 4.14 shows the membership functions for the inputs of ΔP, ΔDi and output Do, normalized in the range of [-1,1]. If ΔP = nm AND ΔDi = nm, then a large duty cycle is commanded, i.e. $Do = ml$, to keep the system on the same course. Defuzzification is the process through which the single output fuzzy set, derived from the aggregation of the outputs of each rule, is converted to a single value. Here, the centroid defuzzification method, which returns as output the center of the area under the curve of the output fuzzy set, is used.

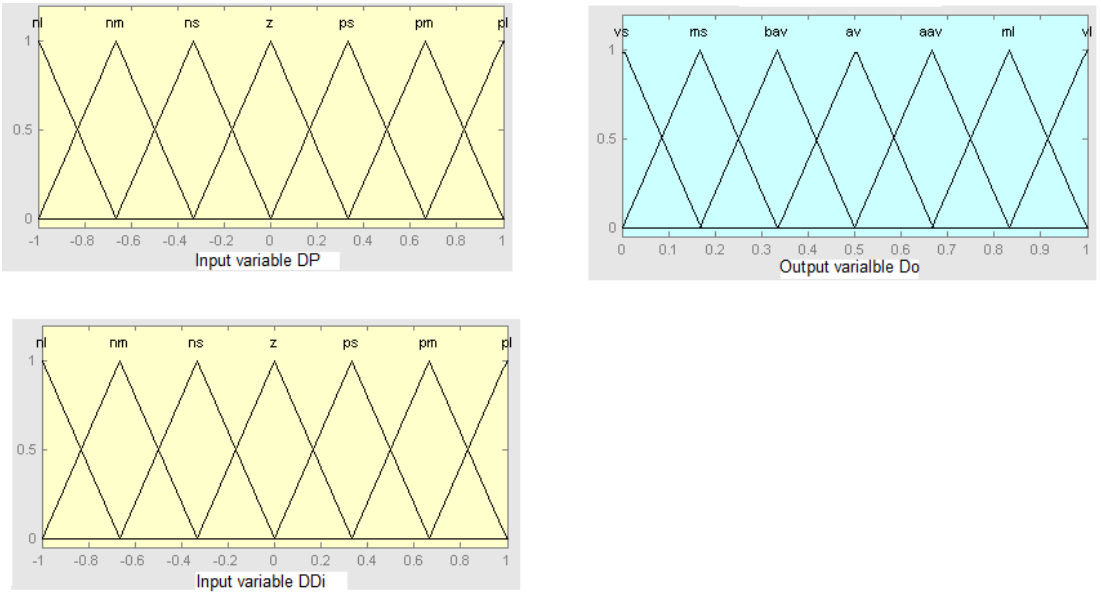

Figure 4.14: Membership functions for fuzzy variables

4.5 FLC based Power management

The Fuzzy Logic Controller is used to control the power generated by wind source, PV source,battery and dump load. Depending on the load demand and available power, the controller selects individual source or combination of sources that will meet the load demand. It will also control the battery state of charge (SOC) by

Table 4.2: Fuzzy rules for wind MPPT

ΔD_n^i	ΔPn						
	nl	**nm**	**ns**	**z**	**ps**	**pm**	**pl**
nl	vl	vl	ml	bav	ms	vs	vs
nm	vl	ml	aav	bav	bav	ms	vs
ns	ml	aav	aav	av	bav	bav	vs
z	vs	ms	bav	av	aav	ml	vl
ps	ms	bav	bav	av	aav	aav	ml
pm	vs	ms	bav	aav	aav	ml	vl
pl	vs	vs	ms	ml	ml	vl	vl

activating the charger control switch when there is excess power from primary sources and activates the discharging switch in case primary sources do not meet the load demand.

The block diagram of fuzzy logic controller based power management is shown in Figure 4.15. In this research, Mamdani type of fuzzy inference is proposed with

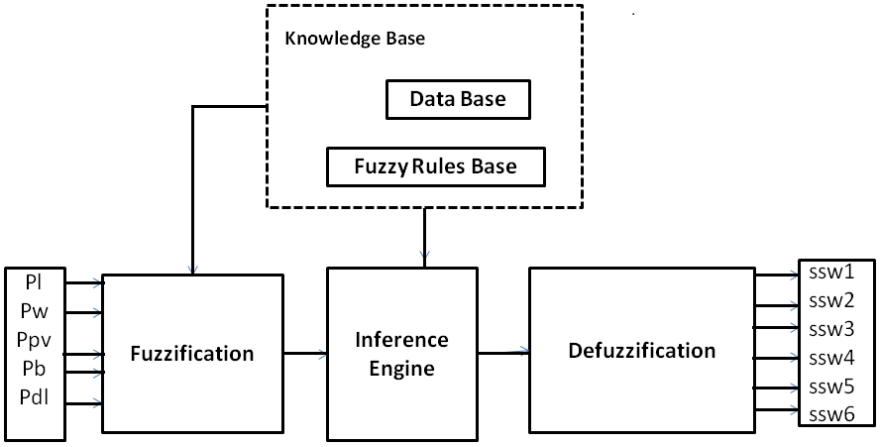

Figure 4.15: Block diagram of fuzzy logic controller for power management

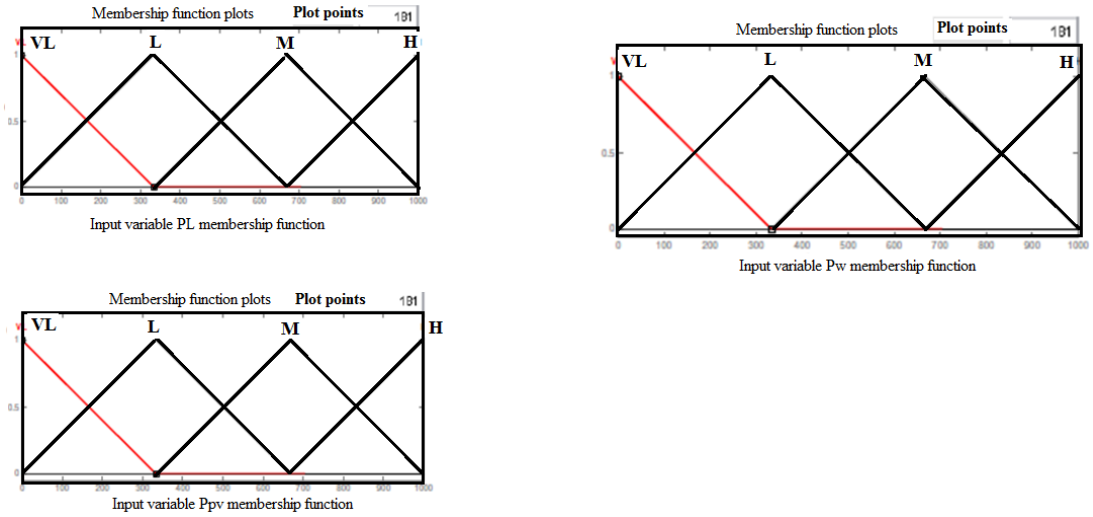

Figure 4.16: Membership functions of input variable

.

Min-Max method of fuzzification and centroid method of defuzzification. The FLC it has 5 inputs named as Pl, Ppv,Pw,Pb and Pdb. It has 6 outputs which are signals for actuating switches such as SSW1, SSW2, SSW3, SSW4, SSW5 and SSW6. All inputs have 4 triangular membership functions namely, Very low, Low, Medium and High (VL, L, M and H) as shown in Figure 4.16. Maximum possible combination of sources under various loads is formed as rules. 21 rules are proposed in this study as shown in Table 4.3. The FLC relates the outputs to the inputs using a list of if-then statements called rules. The if-part of the rules describes the fuzzy sets (regions) of the input variables. In this research, the fuzzy variables Pw, Pl, Pw and Pb are described by fuzzy singleton, i.e. the measured values of these variables are used in the interface process without being fuzzified. Specifically, the fuzzy rules are in the form:

Rule i: IF Pl is Ai and Ppv is Bi and Pw is Ci and Pb is Di, THEN SW1 is Ei and SW2 is Fi and SW3 is Gi and SW4 is Hi and SW5 Ii and SW6 is Ji, where Ai, Bi, Ci and Di are fuzzy subsets in their universes of discourse, and Ei, Fi, Gi, Hi, Ii and Ji are fuzzy singletons. Each universe of discourse is divided into three fuzzy subsets: L (Low), M (Medium), and H (High) and all outputs have

two membership function which are control signals to switch ON and OFF. For the inputs low is defined from 0-200W, medium range from 200-600W and high considered to range from 600-1000w. All selector switches will be off when any of the sources is low. The battery state of charge are limited to between 20% to 80% which means the battery charging switch will be ON only when the state is below 80% and the discharging switch will be ON only when the SOC is above 20%. The FLC is used to decide the optimum operation of the hybrid system, there are six possible operating modes.

1. In single source mode; When any of the renewable sources is sufficient to run the load.
2. In hybrid mode 1;When both renewable sources are sufficient to run the load.
3. In battery mode; When battery alone is sufficient to run the load.
4. In hybrid mode 2; When any one of the renewable source and battery are sufficient to run the load.
5. In Dump load mode; When all the renewable sources and battery are not sufficient, dump load battery will run the load.
6. In off state mode; When battery, Dump load battery and both renewable sources are not sufficient to run the load.

Simulation results and discussions for all modes of operations are presented in Chapter 5.

Table 4.3: Fuzzy rules for power management

Pl	Ppv	Pw	Pb	Pdb	SSWI	SSW2	SSW3	SSW4	SSW5	SSW6
L	L	VL	VL	-	OFF	ON	OFF	OFF	OFF	OFF
L	VL	L	VL	-	ON	OFF	OFF	OFF	OFF	OFF
M	L	L	VL	-	ON	ON	OFF	OFF	OFF	OFF
M	L	VL	M	-	OFF	ON	OFF	ON	OFF	OFF
M	VL	L	M	-	ON	OFF	ON	OFF	OFF	OFF
M	M	VL	VL	-	OFF	ON	OFF	OFF	OFF	OFF
M	VL	M	VL	-	ON	OFF	OFF	OFF	OFF	OFF
M	VL	VL	M	-	OFF	OFF	ON	OFF	OFF	OFF
H	M	H	H	-	ON	ON	ON	OFF	OFF	OFF
H	H	M	H	-	ON	ON	OFF	OFF	OFF	OFF
M	L	VL	L	H	OFF	OFF	OFF	OFF	OFF	ON
M	VL	L	L	H	ON	ON	OFF	OFF	OFF	ON
M	VL	VL	L	H	OFF	OFF	OFF	OFF	OFF	ON
H	L	VL	VL	VL	OFF	OFF	OFF	ON	ON	OFF
H	VL	L	VL	VL	ON	ON	OFF	ON	ON	OFF
H	VL	VL	L	VL	OFF	OFF	OFF	ON	ON	OFF
H	VL	VL	VL	VL	OFF	OFF	OFF	ON	ON	OFF
L	H	H	H	L	ON	ON	OFF	OFF	ON	OFF
H	L	VL	L	H	OFF	OFF	OFF	OFF	ON	OFF
H	VL	L	L	H	ON	ON	OFF	OFF	ON	OFF
H	VL	VL	L	H	ON	OFF	OFF	OFF	ON	OFF

CHAPTER FIVE

RESULTS AND DISCUSSION

This chapter presents a simulation and experimental results of the proposed hybrid system and its control strategy. It includes results for model validation, simulation results for P& O MPPT, Simulation results for ANFIS based MPPT of PV system, simulation results for FLC based wind MPPT and results for FLC based power management.

5.1 Experimental Validation of PV Model

The developed PV model was validated through experimentation by using a simple variable resistive load and Apollo 100-18-P PV module as described in chapter 3. In order to validate the MATLAB/Simulink model, an experiment was performed under different conditions as shown in Table 5.1. This table depicts that

Table 5.1: Comparison of proposed model values with practical values at remarkable points

Remarkable points	**Tilt angle 45 Tc 25 and G 1000**	
	module value	**Practical value**
$Imax$	2.55	2.08
$Vmax$	9.52	11.87
$Pmax$	24.28	24.68

the I-V and P-V simulation and experimental results show a good agreement in terms of current at maximum power point, voltage at maximum power point and maximum power. Moreover error in maximum power is found to be 1.6% which is within the acceptable range of $\pm 3\%$ as specified in the manufacturer datasheet. The simulated and experimental I-V and P-V characteristics of the

solar PV module are shown in Figures 5.1 and 5.2

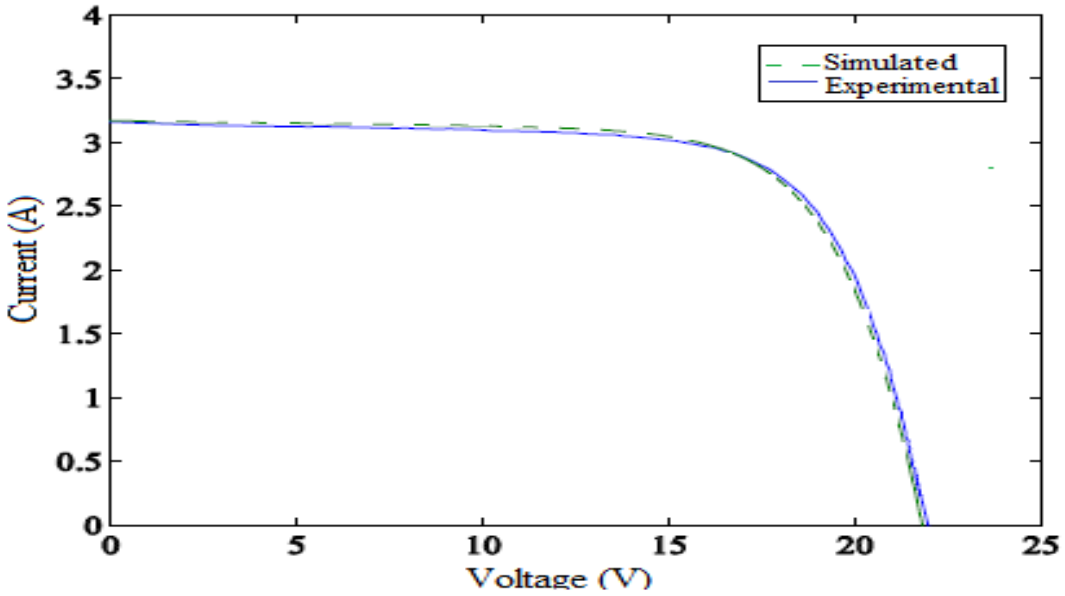

Figure 5.1: Simulated and experimental I-V characteristics of the solar PV module

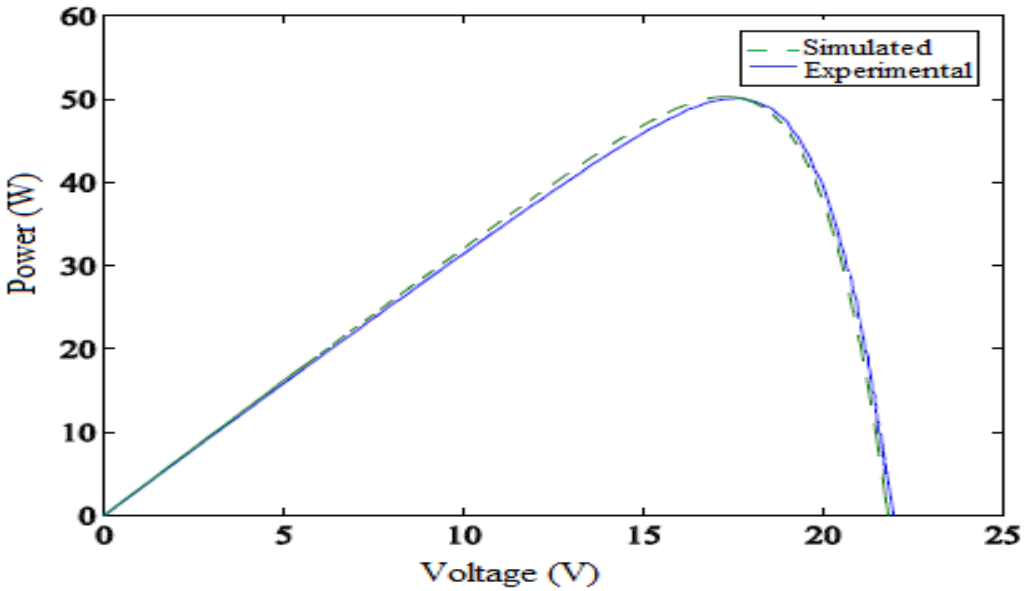

Figure 5.2: Simulated and experimental P-V characteristics of the solar PV module

5.2 Evaluation of proposed PV MPPT

The proposed Simulink model of ANFIS based MPPT control scheme is tested under varying solar irradiance and temperature. Results are compared with the output of PV module when it is connected to the load without MPPT control scheme and with the classical P&O Algorithm. Figure 5.3 shows the dynamic response of the PV output power at constant isolation level of 1000W/m^2 and at constant temperature of 25^oC. As shown from Figure 5.3 The ANN controller shows smoother power signal line, less oscillating and more stable operating point than P&O. It can be seen from the figure that, the ANFIS controller reach the maximum power within 0.3 seconds wheres P&O takes 1.4 seconds to reach the maximum power.From the simulation results, it can be deduced that the ANN controller has better performance than P&O, and it has 4 times accuracy than P&O for operating at MPP.

Figures 5.4 and 5.5 show the dynamic performance of the PV output power at

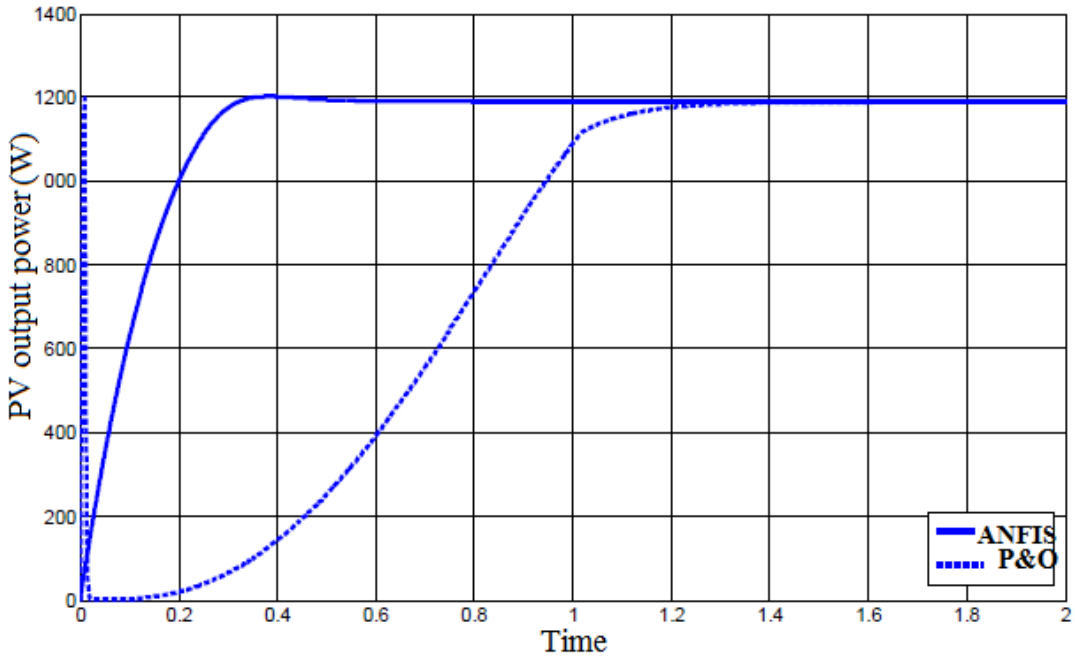

Figure 5.3: PV output power with P & O and ANFIS.

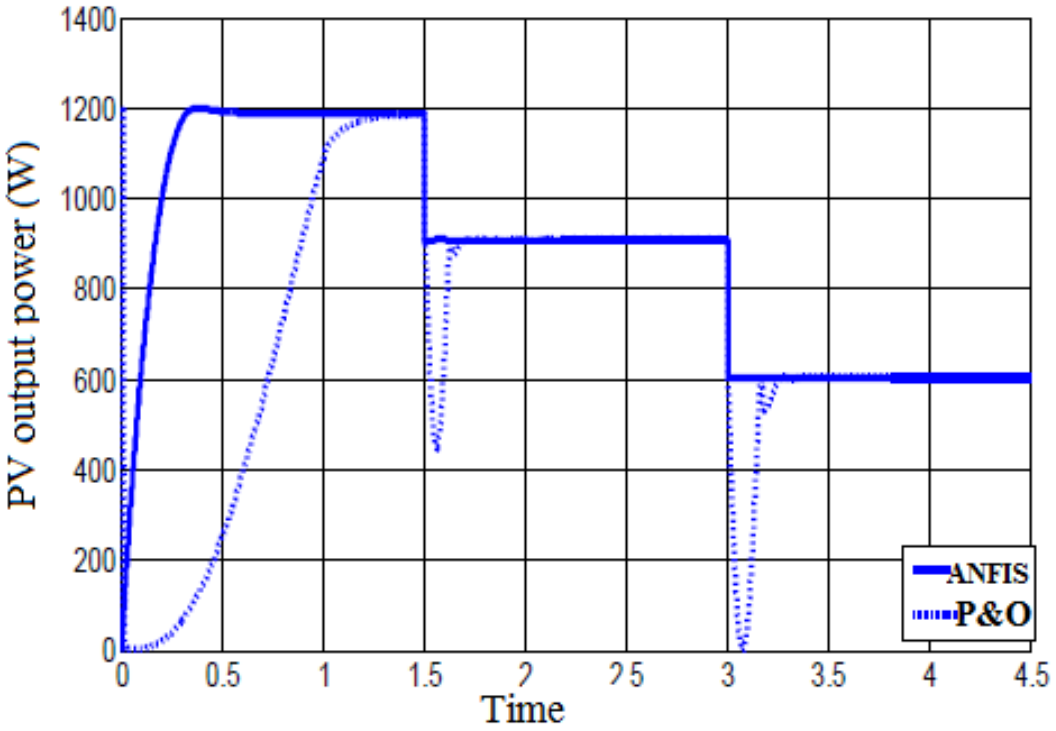

Figure 5.4: PV output power at constant temperature and sudden decrease irradiance level 1000, 750, 500

constant temperature of 25°C and at sudden decrease and increase in irradiance levels, respectively.

Figures 5.4 and 5.5, indicate that while the P&O method fails to track the MPP for fast variations in the irradiance and temperature, the ANN method follow the MPP in short time.

Figure 5.6 shows the response of the PV output power at steady state conditions while the irradiance is low (600W/m^2). Zooming on the curve shows the oscillation of power in case of using the conventional P & O method. These Figures (5.3, 5.4,5.5 and 5.6) indicate that using the FLC method can give the system a very fast response for MPPT (with nearly no oscillations on the MPP at steady state).

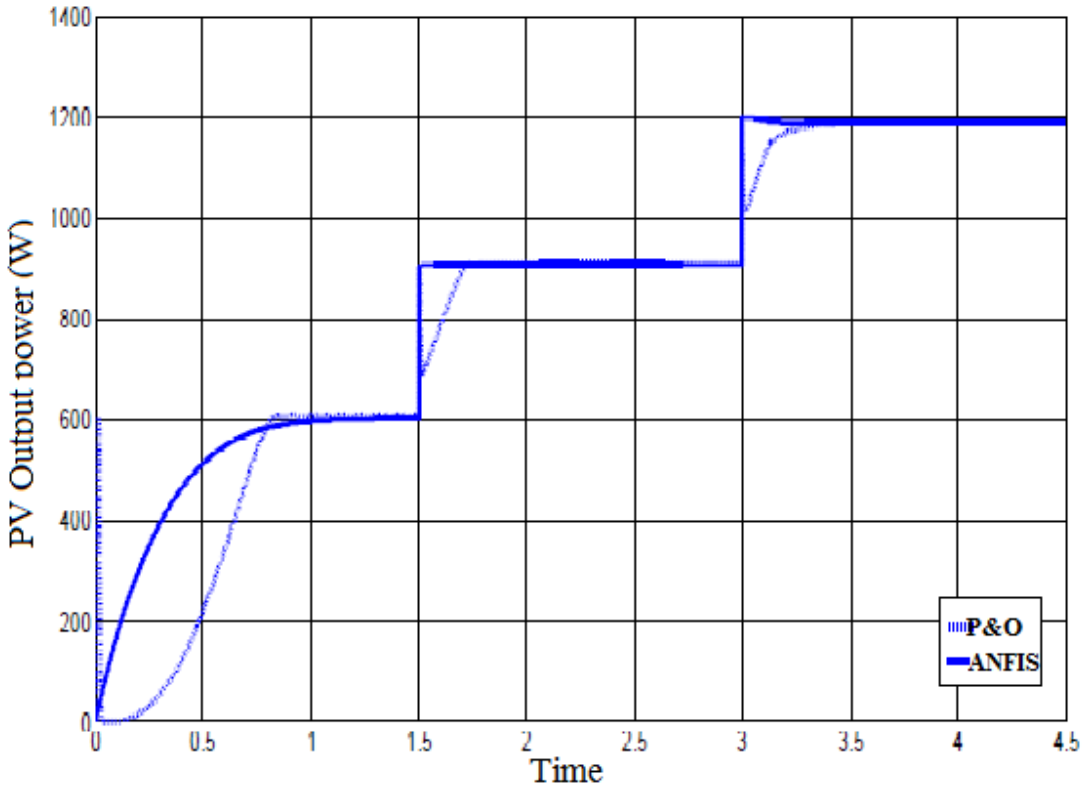

Figure 5.5: PV output power at constant temperature and sudden increase in irradiance level 1000, 750, 500.

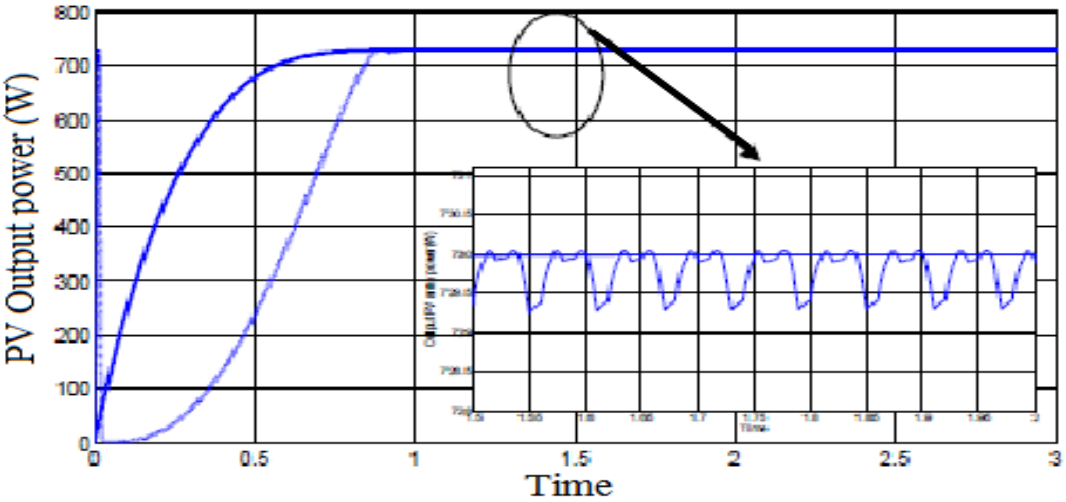

Figure 5.6: PV output power at constant temperature and sudden increase in irradiance level 1000, 750, 500

5.3 Evaluation of proposed FLC based Wind MPPT

The FLC based wind MPPT is simulated using MATLAB/ Simulink. In the simulation, the wind speed changes in three steps. Wind speed at time $t_1 = 0.5s$ and $t_2 = 0.8s$ is changed from 14 m/s to 12 m/s and then reduced to 10 m/s . With the change of wind speed, the performance of wind turbine with fuzzy controller can track the maximum power delivery operating point. Figure 5.7 shows the variation of the wind speed and generator speed. It is seen that according to the wind speed variation, the generator speed varies and that its output power is produced corresponding to the wind speed variation. As was said in literature, Turbine power coefficient is the most important parameter for optimum system performance to obtain the maximum power from the wind. Figure 5.8 shows simulation results of the aerodynamic coefficient Cp.

Figure 5.8 shows that, when the wind speed changes, the wind turbine power coefficient has small fluctuations, but the value of the wind turbine power coefficient quickly changes to the best value. It takes less than $0.2s$ from one stable state to another stable state. The optimal power coefficient value is 0.48, Figure 5.8 demonstrates that, the controller is fast and accurate in performance. Figures 5.9 and 5.10 show the mechanical power and turbine torque curves. It is seen that according to the wind speed variation the mechanical power and turbine torque is produced corresponding to the wind speed variation.

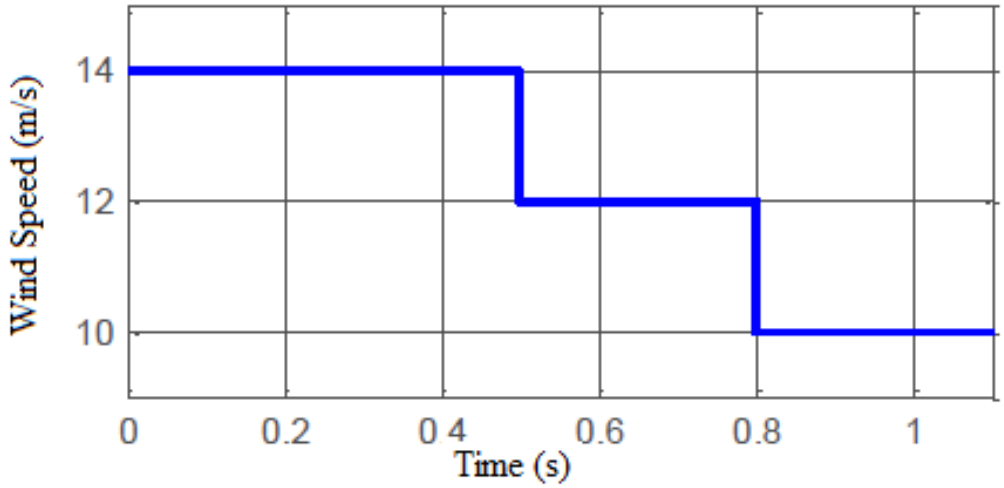

(a) Wind Speed

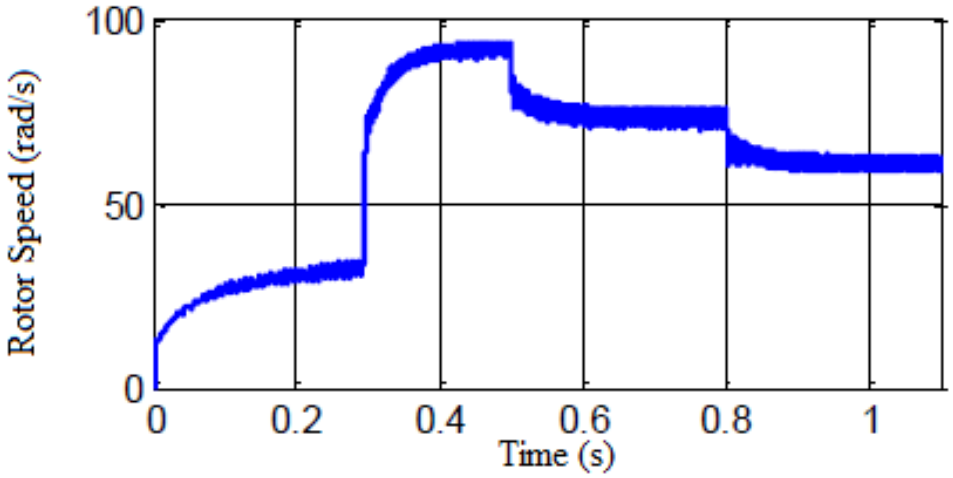

(b) Rotor Speed

Figure 5.7: Simulation results of rotor speed for a step variation of wind speed.

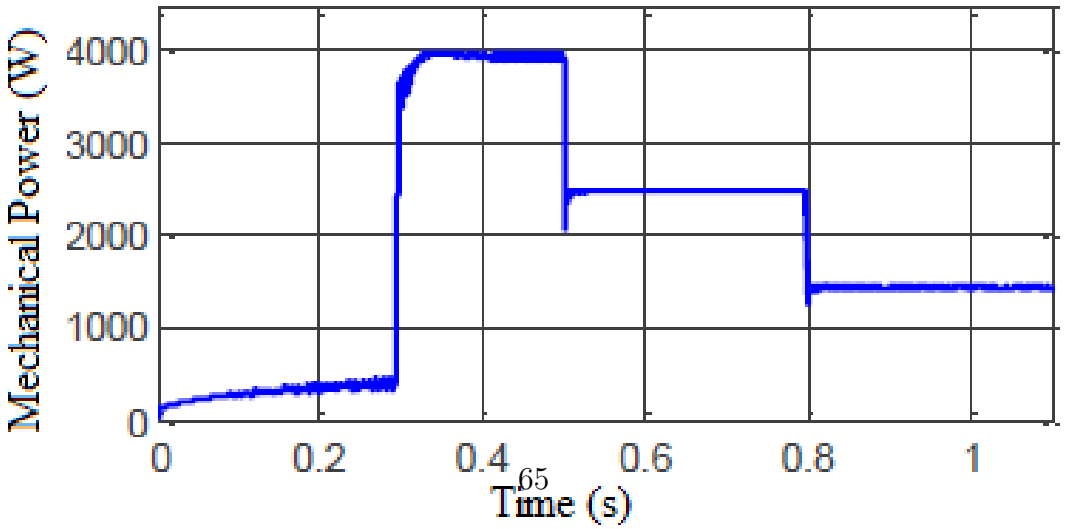

Figure 5.9: The mechanical power curve

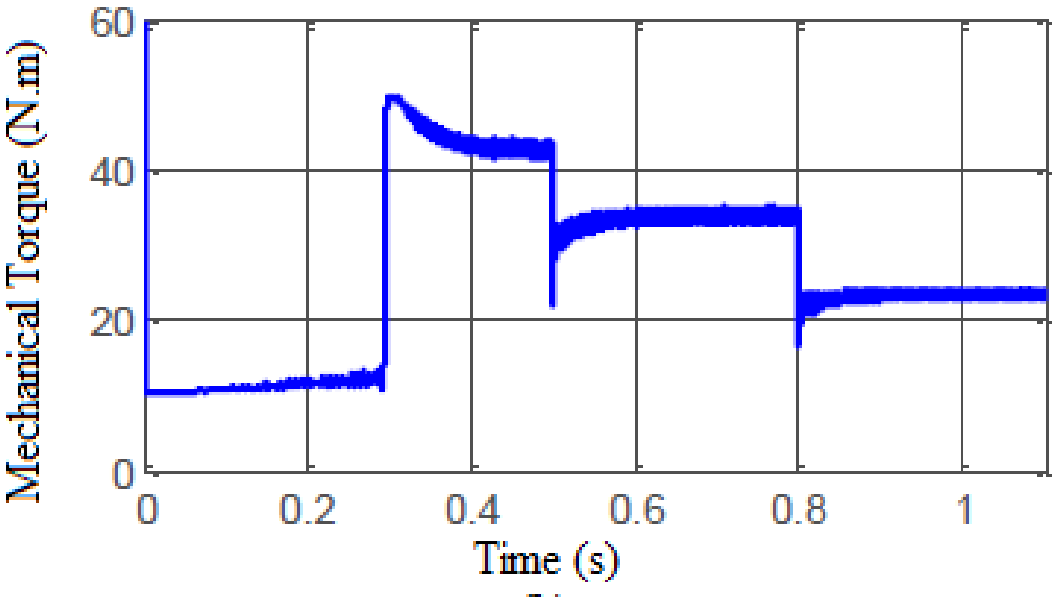

Figure 5.10: Turbine torque curve

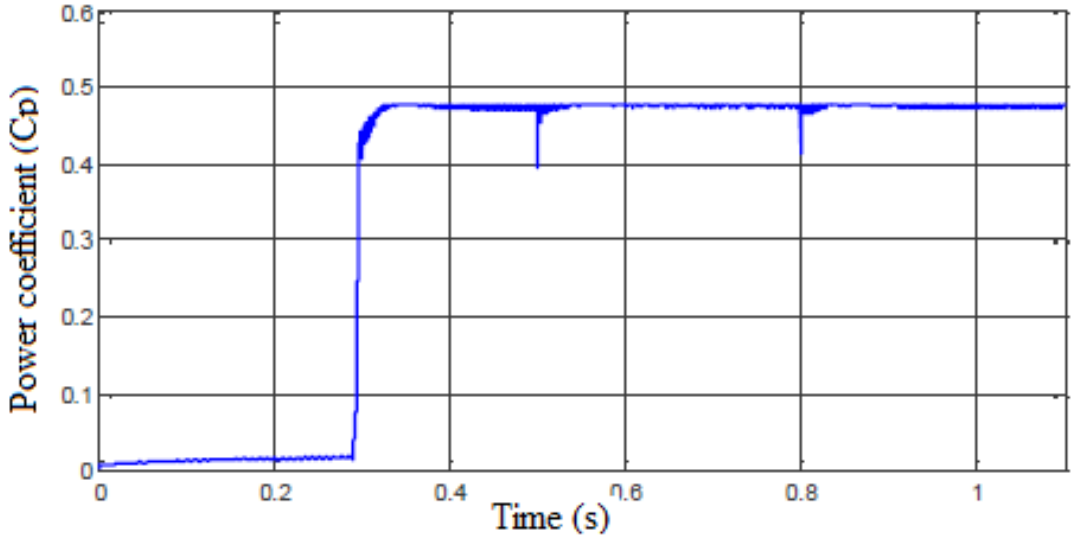

Figure 5.8: Simulation results of aerodynamic constant Cp for three step variation of wind speed

5.4 Results of Simulation for FLC-Based Power Management

Simulation model of PV-Wind hybrid system with battery storage and Fuzzy Logic controller is developed using MATLAB/Simulink software. Rating of hybrid system components is given in Table 5.2. This section presents simulation results of three selected cases for three modes of operation (single source mode, hybrid mode and battery mode) as explained in Chapter 3.

Table 5.2: Rating of hybrid system components

Component	Rating (W)
Wind Power	1500
Pv Power	1500
Battery	3000
Load	2000

Case 1: Single source mode

Figure 5.11 shows the status of a single source supplied load. This is the state where any of the renewable sources is sufficient to run the load. In Figure 5.11, PV alone is sufficient to run the load, PV selector switch (SSW2) is activated and the remaining selector switches are turned off. In the event that the solar power supplied is more than the load demand, the excess power is used to charge the battery through SSW4. The excess power thus activates the charge control SSW4. Fuzzy rule which satisfies this condition is:

"If (Pl is M) and (Ppv is H) and (Pw is VL) and (Pb is VL/L/M) then (SSW1 is ON) and (SSW2 is OFF) and (SSW3 is OFF) and (SSW4 is ON) and (SSW5 is off) and (SSW6 is off)"

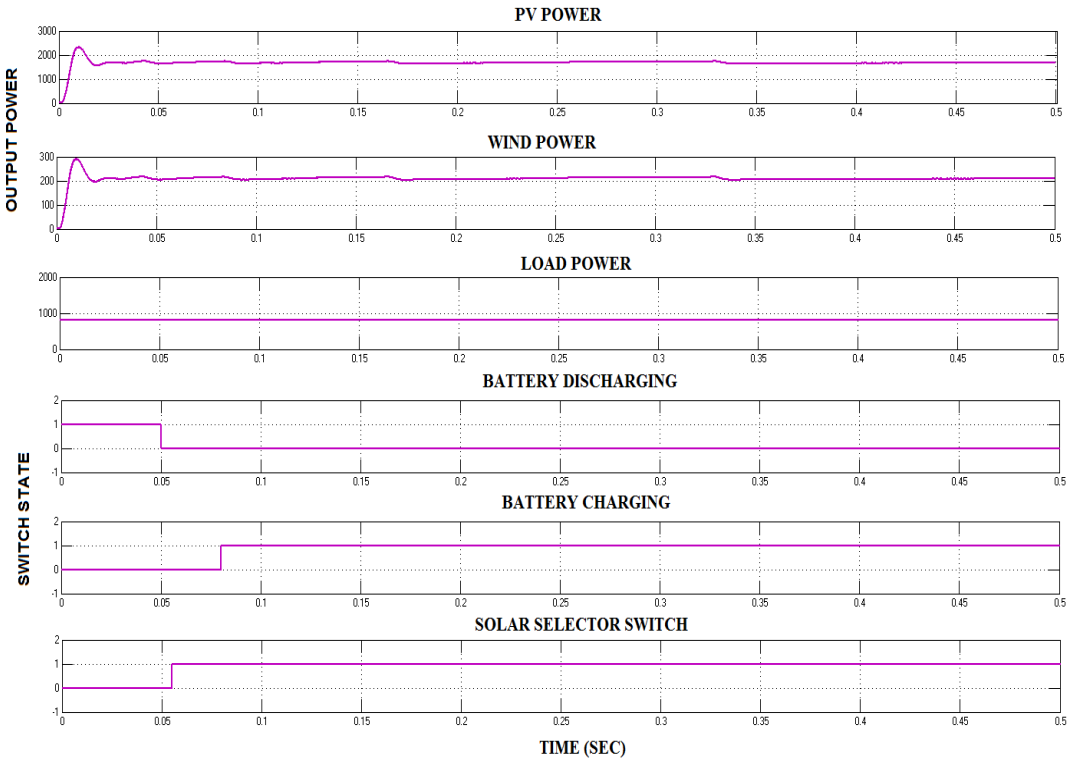

Figure 5.11: Simulation result of the FLC power management when PV power alone supplies load

In Figure 5.11 the power produced by the PV is very high, approximately to its maximum power of 1500w, the power produced by wind is very low, less than 200w while the load demand is high. In this case the PV alone is sufficient to run the load, the excess power from the wind is used to charge the battery through FLC signals to SSW4.

Case 2: In hybrid mode

Here is considered the state where all of the renewable sources are sufficient to run the load. The PV selector switch SSW1, the wind selector switch SSW2, and charge control switches (SSW4 and SSW6) are activated and the other selector switches are turned off. Figure 5.12 shows the response of FLC to this mode of operation.

In Figure 5.12, the power produced by PV and wind is high, the load demand is

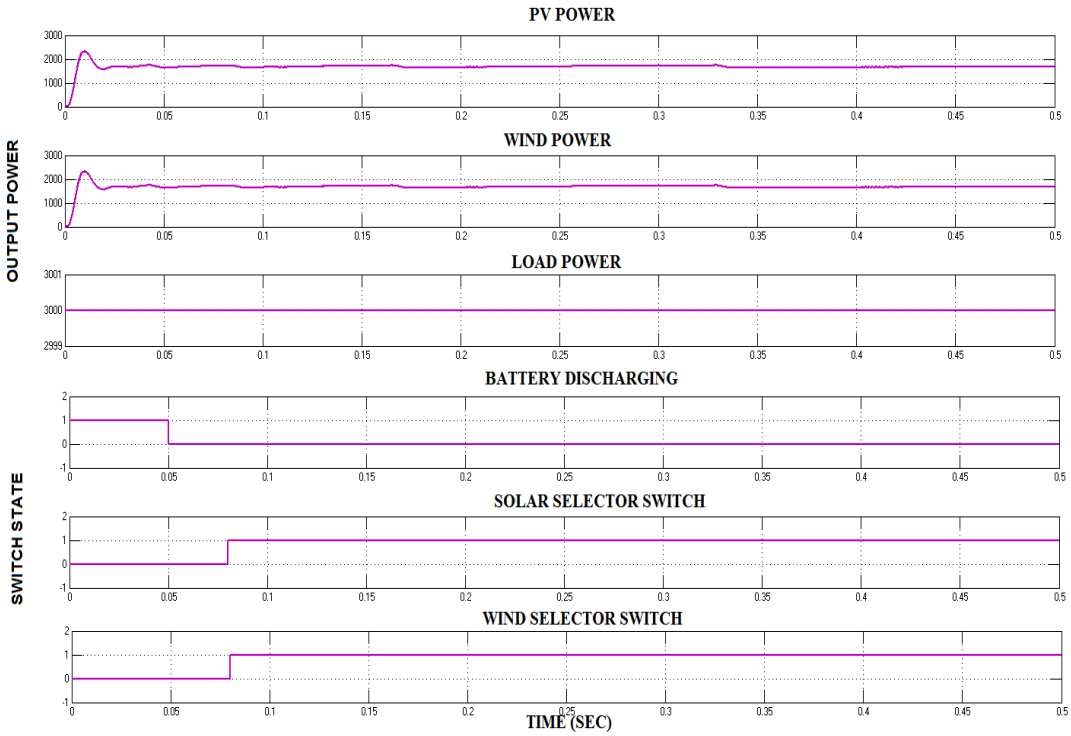

Figure 5.12: Simulation result of the FLC power management when PV and Wind supplies load

also high. In this case the FLC activates the PV selector switch SSW2, the wind selector switch SSW1 and battery charging switches SSW4 and SSW6. Fuzzy rule which satisfies this condition is:

"If (Pl is H) and (Ppv is H) and (Pw is H) and (Pb is VL/L/M) and Pdb is (VL,L,M) then (SSW1 is on) and (SSW2 is on) and (SSW3 is off) and (SSW4 is on) and (SSW5 is off) and (SSW6 is on)"

Case 3: In battery mode 1

Here it consider the state where all of the renewable sources are insufficient to run the load and battery alone is sufficient to run the load. The battery selector switch (SSW4) is activated and remaining selector switches are turned off.

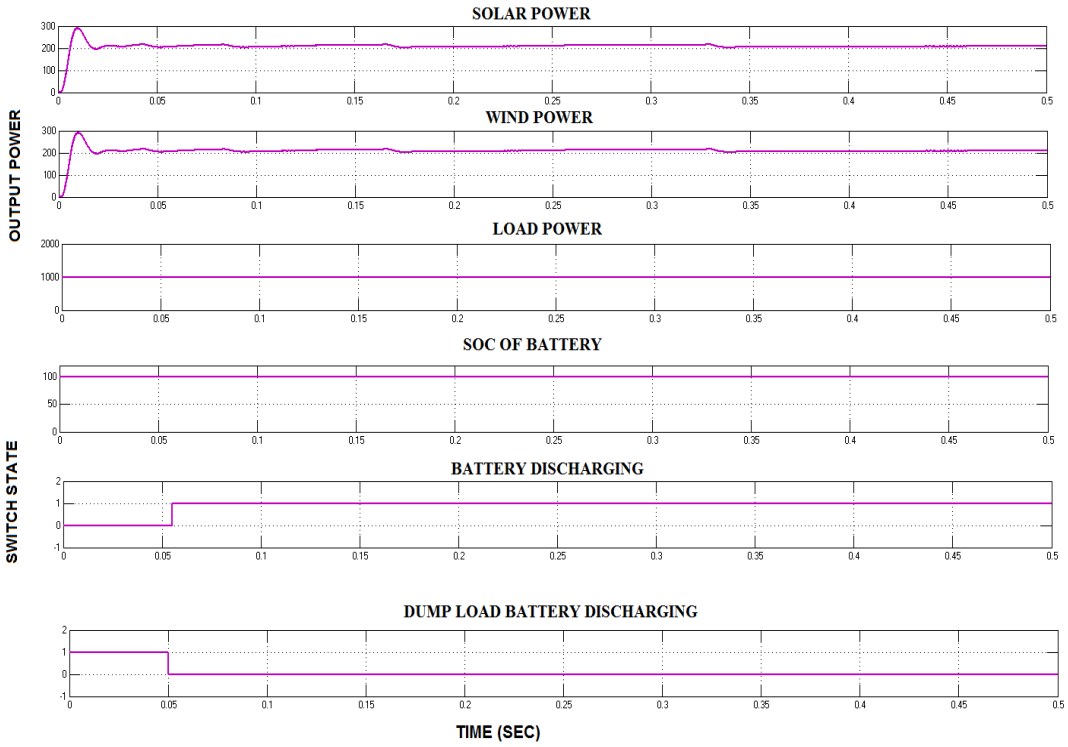

Figure 5.13: Simulation result of the FLC power management when battery alone supplies load

In Figure 5.13, the power produced by PV and wind are very low, the load demand is medium and the battery state of charge is high enough to run the load. In this case the FLC activates the battery discharging switch SSW3 and all the remaining selector switches are turned off. Fuzzy rule satisfying this condition is:

"If (Pl is M) and (Ppv is VL) and (Pw is VL) and (Pb is H) and Pdb is (VL,L,M) then (SSW1 is oFF) and (SSW2 is oFF) and (SSW3 is on) and (SSW4 is off) and (SSW5 is off) and (SSW6 is off)"

CHAPTER SIX

CONCLUSIONS AND RECOMMENDATIONS

6.1 Conclusions

In this study, the block model for the wind power system, PV power system, DC-DC converter, DC-AC converter and the Lead-acid battery were developed and presented in Chapter 3. The photovoltaic model was developed based on its characteristic Equations (2.1), (2.2), (2.3) and (2.4). The proposed model takes cell temperature and solar irradiance as its input parameters and outputs the power under different conditions. The P-V characteristic curves of the PV model under different irradiance (at 25^oC) are given in Figure 3.4 (a). It is concluded that at higher solar irradiance the model gives larger short-circuit current and the open-circuit voltage as the results it gives higher output PV power. It is also concluded that the lower the temperature gives larger open circuit voltage hence gives maximum power.

The wind turbine was modeled using the mathematical equations shown in Chapter 3. In this model, the inputs are the wind speed, pitch angle, and generator speed, the output is the torque applied to the generator shaft. Then the wind turbine model was added with a PMSM which is available in MatLab Simulink library to form the complete wind mode. The FLC for attracting the maximum power was included in the model.This control strategy iscomparatively easy, and has high practical value. From simulation results it is concluded that in any atmospheric conditions such as wind speed changes, the wind turbine system can run stable, and can track the maximum power.

The neural network controller was employed to achieve the MPP for PV panels. Perturb and Observe algorithm was presented for comparison purposes.

The system is simulated in MatLab/Simulink. In the proposed technique the fixed perturbation step size deficiency is overcome through using NNC. Results of comparison of these two controllers in the PV system show adequate and robust performance for the proposed NNC in terms of rise time, settling time and steady state error. Thus, it can be concluded that the NNC enables the PV system to reach the MPP faster and with fewer fluctuations at steady state conditions. This means that the NNC is able to improve the amount of energy extracted from PV module.

The fuzzy logic controller was used to manage the power flow between the hybrid power system and energy storage elements in order to satisfy the load requirements. The controller operates in 6 possible modes: single source mode, hybrid mode, battery mode, dump load mode and off state mode. It can be concluded that the proposed controller provides uninterrupted power, gives effective utilization of sources and minimizing usage of battery hence improves its life time.

6.2 Recommendations

Although the proposed system was proven, by simulation, there are still many areas which could benefit from additional research and development activity before this technology can be feasible for industrial application. Most of these areas are targeted at improving efficiency and increasing overall energy yields. Among them, besides constructing a hardware prototype, photovoltaic/wind turbine monitoring systems. Photovoltaic or wind turbine system owners must be assured that their system operates well and that their investment will pay off. Regardless of which system they operate, plant parks, individual systems or private systems, failures and defects must be detected and repaired immediately. This could be achieved by and only by optimizing these system performance and eliminate any degradation at early stage.

References

[1] Ekren, O., and Ekren, B.(2010). Size optimization of a PV/wind hybrid energy conversion system with battery storage using simulated annealing, *Applied Energy*, *87*(2), 592–598.

[2] Kerr, M., and Cuevas, A. (2004). Generalized analysis of the illumination intensity vs. open-circuit voltage of solar cells, *Solar Energy*, *76*(1-3), 263-267.

[3] Manyonge, R., Ochieng, F., and Shichikha, J. (2012). Mathematical Modeling of Wind Turbine in a Wind Energy Conversion System Power Coefficient Analysis,*Applied Mathematical Sciences*, *6*(2), 4527 - 4536.

[4] Ramu, K., and Rambabu, K. (2014). Renewable Energy Based Small Hybrid Power System For Desalination Applications In Remote Locations,*International Journal of Electrical, Electronics and Data Communication*, *2*(1), 2320-2084.

[5] Ahmed, N., Miyatake, M., and Al-Othman, A.(2008). Power fluctuations suppression of stand-alone hybrid generation combining solar photovoltaic/wind turbine and fuel cell systems, *Energy Conversion and Management*, *49*(10), 2711-2719.

[6] P. Witold, (1993). *Fuzzy control and Fuzzy systems*, studies press ltd, Tauton UK.

[7] Tangka,J. (2012). Development of an Intelligent Electronic Module for Energy Management in Wind/Diesel or Photovoltaic/Diesel Hybrid Systems", *British Journal of Applied Science and Technology*, *2*(3), 275-295.

[8] Yang, H., and Zhou, W. (2007). A novel optimization sizing model for hybrid solar-wind power generation system, *Solar Energy*, *81*(1), 76-84.

[9] Villalva, M., Gazoli J., and Filho, E. (2009). Comprehensive Approach to Modeling and Simulation of Photovoltaic Arrays, *IEEE Transactions on Power Electronics*, *24*(5), 1198-1208.

[10] Ridzuan, M. (2009). Modeling and Simulation of Power Conditioning for Grid-Connected PV/Wind Hybrid Generation System, *Faculty of Electrical Engineering, Universiti Teknologi Malaysia, Johor Bahru.*

[11] Eteiba, M., El Shenawy,T. Shazly H., and Hafez, Z. (2013). A Photovoltaic (Cell, Module, Array) Simulation and Monitoring Model using MATLAB®/GUI Interface, *International Journal of Computer Applications*, *69*(6), 14-28.

[12] Kerr, M., and Cuevas, A. (2003). Generalized analysis of the illumination intensity vs. Open circuit voltage of PV modules. *Solar Energy 76*(1) 263-267.

[13] Borowy, B., and Salameh, M. (1996). Methodology for optimally sizing the combination of a battery bank and PV array in a wind/PV hybrid system, *IEEE Trans Energy Convers*,*11*(2), 367-369.

[14] Zhou, W., Yang H., and Fang, Z. (2007). A novel model for photovoltaic array performance prediction, *Applied Energy*, *84*(12), 1187-1198.

[15] Subudhi, B., and Pradhan, R. A (2013). Comparative Study on Maximum Power Point Tracking Techniques for Photovoltaic Power Systems, *IEEE Transactions on Sustainable Energy*, *4*(1), 89-98.

[16] De Cesare,G., Caputo, D., and Nascetti, A. (2006). Maximum power point tracker for portable photovoltaic systems with resistive-like load, *Solar Energy*,*80*(8), 982-988.

[17] Lim, Y., and Hamill D. (2000) Simple maximum power point tracker for photovoltaic arrays, Electron. *Lett*, *36*(11), 997-1001.

[18] Yang, Y., and Zhao, F. (2011). Adaptive Perturb and Observe MPPT Technique for Grid- Connected Photovoltaic Inverters, *Procedia Engineering,23*(2), 468-473.

[19] Kottas, T., Boutalis, Y., and Karlis, A. (2006). New Maximum Power Point Tracker for PV Arrays Using Fuzzy Controller in Close Cooperation With Fuzzy Cognitive Networks, *IEEE Trans. On Energy Conversion*, *21*(3), 793-803.

[20] Chiu, C. (2010). T-S Fuzzy Maximum Power Point Tracking Control of Solar Power Generation Systems, *IEEE Transactions on Energy Conversion*, *25*, (4), 1123-1132.

[21] Michalke, G., and Hansen, A. (2010). Modelling and control of variable speed wind turbines for power system studies, *Wind Energy*, *13*(4), 307-322.

[22] Manwell, J., McGowan., J. and Rogers, A. (2009). *Wind Energy Explained: Theory, Design and Application.* John Wiley and Sons.

[23] Yang, H., Lu, L., and Zhou, W. (2007). A novel optimization sizing model for hybrid solar-wind power generation system, *Solar Energy,81*(1) 76-84.

[24] Lujano, J., Rojas,R., Dufo, L., and Bernal, J. (2013). Probabilistic modelling and analysis of stand-alone hybrid power systems, *Energy,63* (2), 19-27.

[25] Ekren, B., and Ekren, O. (2009). Simulation based size optimization of a PV/wind hybrid energy conversion system with battery storage under various load and auxiliary energy conditions, *Applied Energy*, *86*(9), 1387-1394.

[26] Zhang, L., Xiong, W., and Xian, X. (2012). Remote Monitoring System Design for Renewable Energy Connected to Power Grid System, *AMR*, *58*(2), 982-985.

[27] Celik, A. (2002). A simplified model based on clearness index for estimating yearly performance of hybrid PV energy systems, *Progress in Photovoltaics: Research and Applications*, *10*(8) 545-554.

[28] Nehrir, M., Lameres, B., Venkataramanan, G., Gerez, V., and Alvarado, L. (2000). An approach to evaluate the general performance of stand-alone

wind/photovoltaic generating systems, *IEEE Transactions on Energy Conversion*, *15*(4), 433-439.

[29] Muljadi, E., and Butterfield, C. (2001). Pitch-controlled variable-speed wind turbine generation, *IEEE Transactions on Industry Applications*, *37*(1), 240-246.

[30] Zamani, M., and Riahy, G. (2008). Introducing a new method for optimal sizing of a hybrid (wind/PV/battery) system considering instantaneous wind speed variations,*Energy for Sustainable Development*, *12*(2), 27-33.

[31] Zhou, W., Yang, H., and Fang, Z. (2008). Battery behavior prediction and battery working states analysis of a hybrid solar–wind power generation system, *Renewable Energy*,*33*(6), 1413-1423.

[32] Cugnet, M., and Liaw, B. (2011). Effect of discharge rate on charging a lead-acid battery simulated by mathematical model, *Journal of Power Sources*, *196*(7), 3414-3419.

[33] De Oliveira, C., and Lopes, M. (2004). Early stages of the lead-acid battery discharge, *Journal of Power Sources*, *138*(1-2), 294-300.

[34] Cugnet, M., and Liaw, B. (2011). Effect of discharge rate on charging a lead-acid battery simulated by mathematical model, *Journal of Power Sources*, *196*(7), 3414-3419.

[35] Bernardi, D. (1995). A Mathematical Model of the Oxygen-Recombination Lead-Acid Cell, *J. Electrochem. Soc.*, *142*(8), 2631.

[36] Nguyen, T. (1990). The Effects of Separator Design on the Discharge Performance of a Starved Lead-Acid Cell, *J. Electrochem. Soc.*, *137*(10), 2998.

[37] Piller,S., Perrin M., and Jossen, A. (2001). Methods for state-of-charge determination and their applications, *Journal of Power Sources*, *96*(1), 113-120.

[38] Borowy, B., and Salameh, Z. (1996). Methodology for optimally sizing the combination of a battery bank and PV array in a wind/PV hybrid system, *IEEE Trans. On energy Conversion*, *11*(2),367-375.

[39] Deshmukh, M., and Deshmukh, S. (2008). Modeling of hybrid renewable energy systems, *Renewable and Sustainable Energy Reviews*, *12*(1) 235-249.

[40] Reddy, K. and Agarwal, V. (2007). Utility-Interactive Hybrid Distributed Generation Scheme With Compensation Feature, *IEEE Trans. On Energy Conversion*, *22*(3), 666-673.

[41] Natsheh, E., Albarbar A., and Yazdani, J. (2011). Modeling and Control for Smart Grid Integration of Solar/Wind Energy Conversion System ,*Innovative Smart Grid Technologies (ISGT Europe).*

[42] Rao, Y., Laxmi, A., and Kazeminehad, M. (2012). Modeling and control of hybrid photovoltaic wind energy conversion system,*International Journal of Advances in Engineering & Technology.*

[43] Meng, O., and Altas, I. (2012). Fuzzy logic control for a wind/battery renewable energy production system, *Turk J Elec Eng & Comp Sci*, *20*(2).

[44] Shah, S. Intelligent Algorithms for a Hybrid Fuel Cell/Photovoltaic Standalone System, (2010). *Msc, Dalarna University.*

[45] Jurado, F., and Saenz, J. (2003). An adaptive control scheme for biomass-based diesel–wind system, *Renewable Energy*, *28*(1), 45-57.

[46] Dorz, R., and Pius, S. (2012). ANFIS based Neuro-Fuzzy Controller in LFC of Wind-Micro Hydro-Diesel Hybrid Power System, *International Journal of Computer Applications*, *42*(6), 28-35.

[47] Ko, H., Lee, K., Kang M., and Kim, H. (2008). Power quality control of an autonomous wind–diesel power system based on hybrid intelligent controller, *Neural Networks*, *21*(10) 1439-1446.

[48] Robyn, A. (2007). A Simple, Effective Lead-Acid Battery Modeling Process for Electrical System Component Selection, *The MathWorks, Inc.*

[49] Atieno, L. (2013). Optimization of fuel consumption in hybrid Wind-Diesel system using fuzzy logic controller, *Unpublished Msc thesis,Juja Jomo Kenyatta University of Agriculture and Technology.*

Appendix 1 Structure of a Fuzzy Logic Controller Fuzzy control is based on fuzzy logic, a concept developed by Lotfi Zadeh in 1965 to evaluate, analyse and control systems with vague, imprecise and/or incomplete variables. According to Zadeh, as the complexity of a system increases, one's ability to make precise and yet significant statements about its behaviour diminishes until a threshold is reached beyond which precision and significance become almost mutuFally exclusive characteristics [31].This is known as the principle of incompatibility.

Since many natural systems incorporate imprecise and incomplete data, fuzzy logic is a powerful tool for controlling such systems. One of the strengths of fuzzy logic based techniques is the use of natural language in the definition of the input variables, the construction of the logic rules and the generation of outputs. Thus, as a soft computing technique, fuzzy control is tolerant to suboptimality and impreciseness, and gives quick, simple and sufficiently good solutions [32].

The main advantage of fuzzy logic controllers (FLCs) is their ability to incorporate experience and heuristics into the system instead of relying on mathematical models. Heuristics are approximations used in problem solving which trade optimality, completeness, accuracy and/or precision for speed, and can be compared to a "best guess". Due to the incorporation of experience and heuristics, FLCs are thus more effective in applications where existing models are ill defined or are not reliable enough [33].

An overall representation of a fuzzy logic controller is shown in Figure 6.1, and indicates the stages in fuzzy logic control.

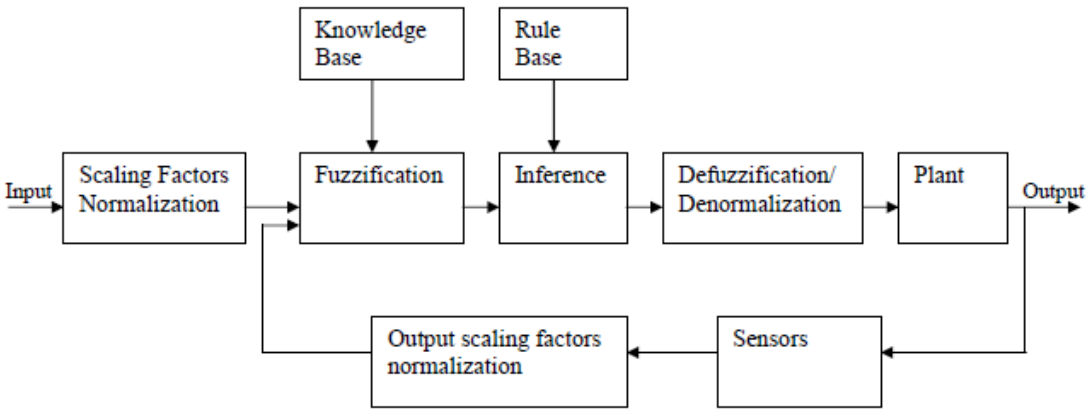

Figure 6.1: Fuzzy control block diagram

A fuzzy logic controller consists of type main elements:

1. Fuzzification module/ fuzzifier.
2. Knowledge base.
3. Rule base.
4. Inference engine.
5. Defuzzification module.

Automatic changes in design parameters of any of the type elements creates an adaptive FLC. This means that the controller is able to automatically change in reaction to system conditions, such that for the same initial controller employed under different system conditions, after a while, the design parameters of the controller are found to have changed, or adapted, to the system. Controllers with fixed parameters are referred to as non-adaptive. Other non-fuzzy elements include sensors, analogue-digital converters (ADCs), digital-analogue converters(DACs) and normalization circuits.

6.3 Fuzzifier

The fuzzifier converts real world crisp values into fuzzy variables to enable manipulation by the FLC. This is referred to as fuzzification, and involves input from the knowledge base.

6.4 Knowledge Base

The knowledge base is a database of the plant, and defines relationships necessary for the fuzzifcation process, such as definition of the membership functions, fuzzy set representation of input and output variables and relationships between physical and fuzzy representations of variables.

A membership function (MF) is a curve that defines how each point in the input space is mapped to a membership value (or degree of membership) between 0 and 1. The input space is sometimes referred to as the universe of discourse.

Membership functions take various shapes, with the most commonly used being triangular and trapezoidal shapes to reduce complexity in calculations. Other avail- able shapes include gaussian, sigmoid, pi-shaped, s-shaped, as well as user-defined functions. A selection of membership function shapes is shown in Figure 6.2.

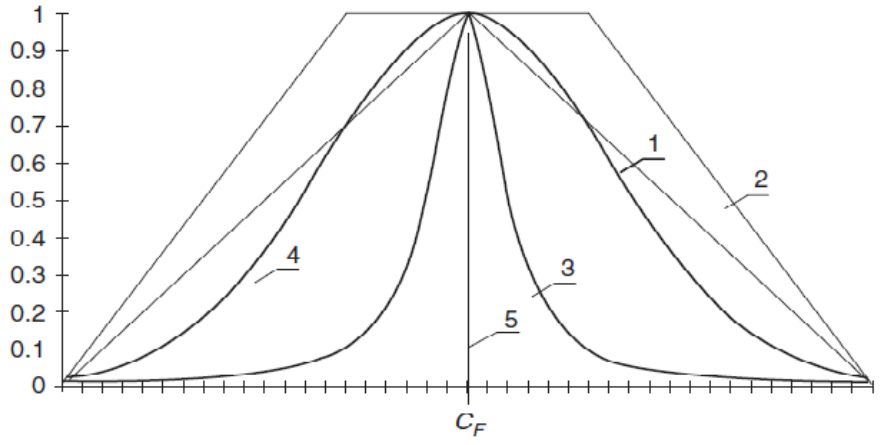

Figure 6.2: Membership function curves

The assignment of values within the membership functions can be done using one of six common methods:

1. **Intuition:** Is derived from the human capacity to develop membership functions through their own innate knowledge and understanding. It involves con- textual and semantic knowledge about an issue, and may also involve linguistic truth values about this knowledge.

2. **Inferencing:** In this method, available knowledge is used to perform deductive reasoning. One uses a body of available facts or knowledge to deduce or infer a set of membership functions.

3. **Rank Ordering:** Preferences by a single individual, a committee or poll or other opinion methods are assessed and membership values assigned based on pairwise comparisons. This method requires use of data collection methods such as questionnaires, and appropriate data analysis techniques to come up with useful ranking data that can be used to generate membership functions for FLC.

4. **Neural Networks:** A neural network builds an intelligent program model that simulates the working network of neurons in the human brain. This allows for learning (and in some cases, forgetting), thus the membership functions are generated through a process that involves gradual improvement until an optimal solution is obtained.

5. **Genetic Algorithms:** This method allows for searching for an optimal solution from a nearly infinite set of possible solutions using a process that mimics the genetic model of "survival of the fittest", involving reproduction, crossover and mutation of solutions until an acceptable solution is arrived at, with all unfit solutions abandoned during the process.

6. **Inductive Reasoning:** This method involves deriving a general consensus from the particular, and is useful where large volumes of static data are avail- able. Membership functions are generated from input-output relationships inferred from the database.

Once the membership values have been assigned, the membership functions are generated by repeated partitioning of the data range.

6.5 Rule Base

The rule base is used to determine the outputs that correspond to a given input or set of inputs. Fuzzy rules are expressed as IF...THEN rules, with different inputs being related to each other using logical operators AND and OR as well as NOT. The rule base may be obtained from expert knowledge or from heuristics.

The fuzzy rule has two important parts, the antecedent, which describes the input condition(s) for which the rule is to be used and the consequent, which is the resultant output. Some controllers include a weight for each output, which is a factor that indicates the relative contribution of the particular rule to the overall output.

6.6 Inference Engine

When a particular rule is activated as a result of its antecedent being greater than 0, the rule is said to be fired. Since in general, crisp values tend to fire more than one rule, unless they occur at the boundary points of fuzzy subsets, the resultant output consists of several different output variables with different degrees of membership. These outputs need to be processed to give a single expression of the output in terms of the fuzzy membership functions that will proceed to

defuzzification, to produce a single crisp output. This is known as aggregation. The inference engine provides the implication or aggregation technique that will be used to interpret the fuzzy rules. The most common methods used in aggregation are Mamdani method and Sugeno method.

The Mamdani inference method aggregates the output membership functions in terms of area covered, and the overall output is a 2-dimensional shape that expresses the total contribution of each fired output. The Sugeno inference method expresses each output as a singleton, and the resultant aggregate is also expressed as a singleton, with its position determined by the defuzzification method used. An overview of the processing involved using a Mamdani type controller is given in the inference diagram shown in Figure 6.3.

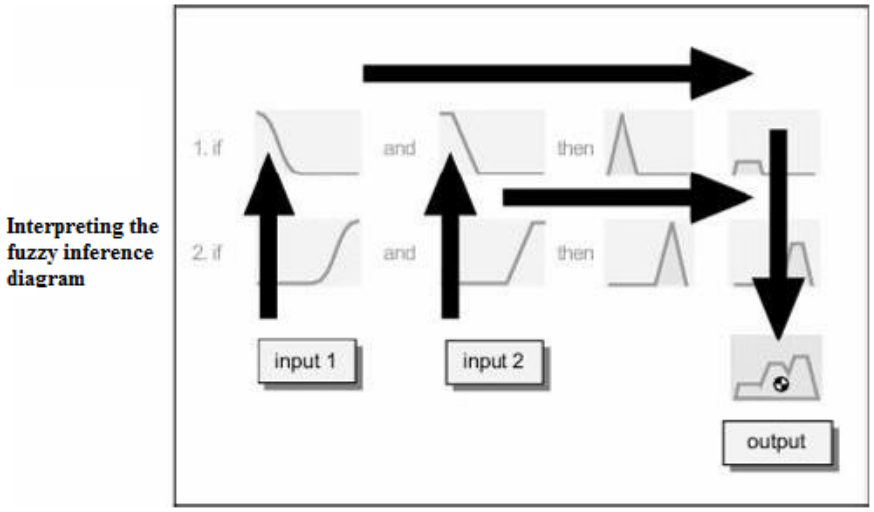

Figure 6.3: Inference diagram

6.7 Defuzzifier

The defuzzifier converts the fuzzy output obtained from the inference engine into a crisp value that can be used by the plant as a control signal. The most common defuzzification method is the centre of gravity method, also known as the centroid method. Other less commonly used methods include centre of maximum, largest

of maximum and smallest of maximum.

In the centroid method, the centre of gravity of the 2-dimensional shape or the singleton obtained from aggregation is obtained, and related to a crisp output on the output membership function. This value is the output of the FLC.

In general, the crisp output from the defuzzifier, using the centre of gravity method, is expressed as:

$$f(y) = \frac{\sum_{m=1}^{n} E^m . D^m}{\sum_{m=1}^{n} D^m} \tag{6.1}$$

where: $f(y)$ is the crisp output value

E^m is the crisp weighting value for the linguistic variable whose output is being determined. D^m is the membership value of y with relation to the linguistic variable.

Appendix 2 Architecture of an Artificial Neural Network

Artificial neural network has a form of multiprocessor computing system. It consists of a number of very simple and highly interconnected processors, called neurons, which are analogous to the biological neurons in the brain. The basic model of a single neuron is shown in Figure 6.4.

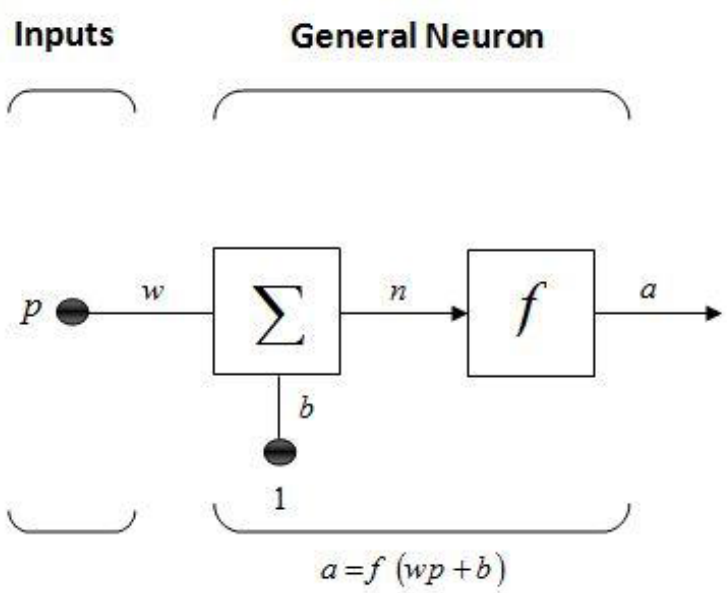

Figure 6.4: Architecture of a single artificial neuron

Figure 6.4 shows a single artificial neuron with an input vector p , a connection weight vector w, a bias b , an activation function f and an output a . The output (a) of this neuron is defined as follows:

$$a = f(\mathbf{p}.\mathbf{w} - \mathbf{b}) = \mathbf{f}\sum_{\mathbf{n=1}}^{\mathbf{N}} \mathbf{P_n}.\mathbf{w_n} - \mathbf{b}, = \forall \mathbf{p} = \begin{pmatrix} p_1 \\ \vdots \\ \vdots \\ p_N \end{pmatrix}, \forall \mathbf{w} = \begin{pmatrix} w_1 \\ \vdots \\ \vdots \\ p_N \end{pmatrix} \qquad (6.2)$$

The effect of the bias b on the activation function f is a shift to the left or the right, depending on whether it is positive or negative. The activation function f can be taken from a set of activation functions (as piecewise-linear function, hard

limit function, sigmoid function). Some of the most popular activation functions are shown in Figure 6.5

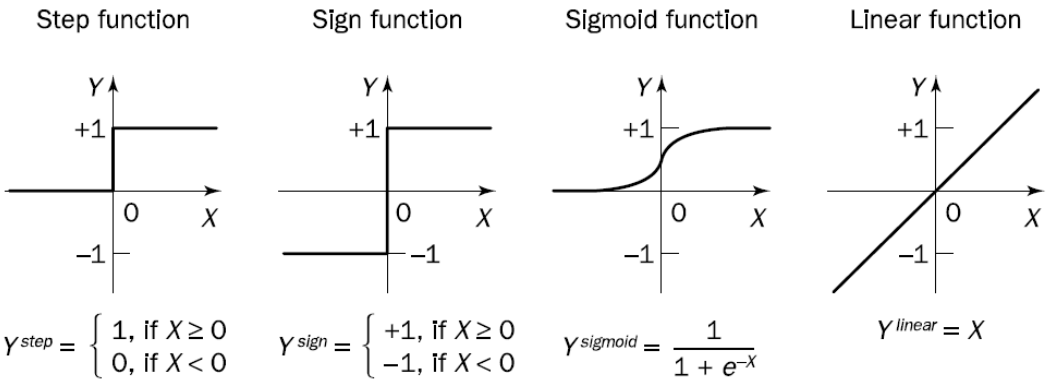

Figure 6.5: Popular activation functions used in ANN

Using this basic model of a neuron as shown in Figure 6.5, different ANN architectures have evolved, among them feed-forward neural network. Feed-forward ANNs allow signals to travel in one way only; from inputs to outputs. They are extensively used in nonlinear system modeling. The earliest kind of neural network is a single layer perceptron network which consists of a single layer of output nodes; the inputs are fed directly to the outputs via a series of weights. In this way it can be considered the simplest kind of feed-forward network.

The next popular feed-forward model, as shown in Figure 6.6, is the multi-layer perceptron. It is a feed forward neural network model that maps sets of input data onto a set of outputs. It has more than two layers. The layers are fully connected. So that, every neuron in each layer is connected to every other neuron in the adjacent forward layer.

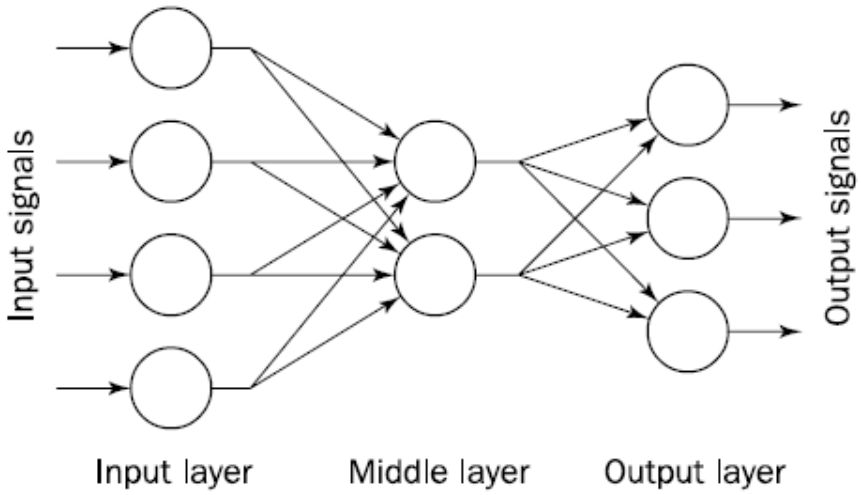

Figure 6.6: Architecture of a multilayer perceptron

A neuron determines its output in a way similar to Rosenblatt's perceptron First, it computes the net weighted input:

$$X = \sum_{i=1}^{n} X_i w_i - \theta \tag{6.3}$$

Where n is the number of inputs and θ is the threshold applied to the neuron. Next, this input value is passed through the activation function. Multi-layer networks use a variety of learning techniques, the most popular being back-propagation. In back-propagation, the learning law has two phases. First, a training input pattern is presented to the network input layer. The network then propagates the input pattern from layer to layer until the output pattern is generated by the output layer. If this pattern is different from the desired output, an error is calculated and then propagated backwards through the network from the output layer to the input layer. The weights are modified as the error is propagated.

6.8 Adaptive Neural Fuzzy Inference System

An adaptive neuro-fuzzy inference system or adaptive network-based fuzzy inference system (ANFIS) is a kind of artificial neural network that is based on Takagi–Sugeno fuzzy inference system. The technique was developed in the early 1990s. Since it integrates both neural networks and fuzzy logic principles, it has potential to capture the benefits of both in a single framework. Its inference system corresponds to a set of fuzzy IF–THEN rules that have learning capability to approximate nonlinear functions. Hence, ANFIS is considered to be a universal estimator.

Appendix 3 Training data for the ANFIS

Table 6.1: Training data for the ANFIS.

Irradiance	Temperature	Voltage	Irradiance	Temperature	Voltage
100	15	21.22	600	40	18.94
150	15	21.69	650	40	18.95
200	15	22	700	40	18.96
250	15	22.21	750	40	18.96
300	15	22.37	800	40	18.96
350	15	22.49	850	40	18.95
400	15	22.58	900	40	18.93
450	15	22.65	950	40	18.91
500	15	22.71	1000	40	18.88
550	15	22.74	100	45	16.48
600	15	22.77	150	45	17
650	15	22.79	200	45	17.33
700	15	22.8	250	45	17.57
750	15	22.8	300	45	17.74
800	15	22.8	350	45	17.87
850	15	22.79	400	45	17.97
900	15	22.78	450	45	18.05
950	15	22.76	500	45	18.1
1000	15	22.74	550	45	18.14
100	20	20.43	600	45	18.17
150	20	20.91	650	45	18.19
200	20	21.22	700	45	18.19
250	20	21.44	750	45	18.19
300	20	21.6	800	45	18.19
350	20	21.72	850	45	18.18

400	20	21.82	900	45	18.16
450	20	21.89	950	45	18.14
500	20	21.94	1000	45	18.11
550	20	21.98	100	50	15.68
600	20	22.01	150	50	16.21
650	20	22.02	200	50	16.55
700	20	22.03	250	50	16.79
750	20	22.04	300	50	16.97
800	20	22.03	350	50	17.1
850	20	22.02	400	50	17.2
900	20	22.01	450	50	17.28
950	20	21.99	500	50	17.33
1000	20	21.92	550	50	17.37
100	25	19.64	600	50	17.4
150	25	20.13	650	50	17.42
200	25	20.45	700	50	17.42
250	25	20.67	750	50	17.42
300	25	20.83	800	50	17.42
350	25	20.96	850	50	17.41
400	25	21.05	900	50	17.39
450	25	21.12	950	50	17.37
500	25	21.17	1000	50	17.34
550	25	21.21	100	55	14.89
600	25	21.24	150	55	15.43
650	25	21.26	200	55	15.77
700	25	21.27	250	55	16.02
750	25	21.27	300	55	16.2
800	25	21.26	350	55	16.33

850	25	21.25	400	55	16.43
900	25	21.24	450	55	16.51
950	25	21.22	500	55	16.56
1000	25	21.2	550	55	16.6
100	30	18.85	600	55	16.63
150	30	19.35	650	55	16.65
200	30	19.67	700	55	16.66
250	30	19.9	750	55	16.66
300	30	20.06	800	55	16.65
350	30	20.19	850	55	16.64
400	30	20.28	900	55	16.62
450	30	20.35	950	55	16.59
500	30	20.41	1000	55	16.57
550	30	20.44	100	60	14.09
600	30	20.47	150	60	14.64
650	30	20.49	200	60	14.99
700	30	20.5	250	60	15.24
750	30	20.5	300	60	15.42
800	30	20.49	350	60	15.56
850	30	20.48	400	60	15.66
900	30	20.47	450	60	15.73
950	30	20.45	500	60	15.79
1000	30	20.43	550	60	15.83
100	35	18.06	600	60	15.86
150	35	18.57	650	60	15.88
200	35	18.89	700	60	15.89
250	35	19.12	750	60	15.89
300	35	19.29	800	60	15.88

350	35	19.42	850	60	15.87
400	35	19.51	900	60	15.85
450	35	19.58	950	60	15.82
500	35	19.64	1000	60	15.8
550	35	19.68	100	65	13.3
600	35	19.7	150	65	13.85
650	35	19.72	200	65	14.21
700	35	19.73	250	65	14.46
750	35	19.73	300	65	14.64
800	35	19.73	350	65	14.78
850	35	19.71	400	65	14.89
900	35	19.7	450	65	14.96
950	35	19.68	500	65	15.02
1000	35	19.65	550	65	15.06
100	40	17.27	600	65	15.09
150	40	17.78	650	65	15.11
200	40	18.11	700	65	15.12
250	40	18.35	750	65	15.12
300	40	18.52	800	65	15.11
350	40	18.65	850	65	15.1
400	40	18.74	900	65	15.08
450	40	18.82	950	65	15.05
500	40	18.87	1000	65	15.02
550	40	18.91			